Coexistence in Periodic Environments

Alexa M Scott[1*], Carling Bieg[1], Bailey C McMeans[2], Kevin S McCann[1]

[1] Department of Integrative Biology, University of Guelph, Ontario, Canada

[2] Department of Biology, University of Toronto, Mississauga, Ontario, Canada

*corresponding author

ORCIDs and email addresses

*Alexa M Scott: 0000-0003-0776-0582 (ascott16@uoguelph.ca)

Carling Bieg: 0000-0003-1552-2007 (cbieg@uoguelph.ca)

Bailey C McMeans: 0000-0002-9793-6811 (bailey.mcmeans@utoronto.ca)

Kevin S McCann: 0000-0001-6031-7913 (ksmccann@uoguelph.ca)

Keywords: Periodicities, species coexistence, competition, Lotka-Volterra, climate change

Word Count: 5260 (main body)

Submission Content: Main text, one table, six figures, supplementary material (5 sections)

Abstract

Theoretical knowledge on the ecological significance of periodic environments is still underdeveloped. Despite this, many global periodicities – on a variety of timescales – are changing due to climate change and other anthropogenic impacts. Thus, alterations in these periodicities may fundamentally restructure species interactions and future competitive outcomes, with clear implications for the maintenance of biodiversity under global change. We extend a two-species Lotka-Volterra competition model that incorporates periodic forcing between two seasons of high and low productivity to investigate the effects of changing environmental patterns on species coexistence. Towards this, we define coexistence criteria for periodic environments by approximating isocline solutions akin to classical coexistence outcomes. This analytical approach illustrates that seasonality can mediate different competitive outcomes, and that our numerical results and bifurcation patterns are quite general. Importantly, species coexistence may be incredibly sensitive to changing periodicities, and therefore, climate change has the potential to drastically impact the maintenance of biodiversity in the future.

Introduction

Nature is abundant with a diverse array of periodic climate signals (Jackson et al. 2021; Pokorný 2021). The complex variations in temperature over time (Litchman and Klausmeier 2001; Jiang and Morin 2007; Rudolf 2019), for example, can be decomposed into different lengths of underlying periodicities using spectral analysis, revealing a complex mosaic of short (e.g., seconds, minutes, hours, days), medium (months, years), long (multi-decadal), and very long natural periods (100s to 1000s of years) (Forrest and Miller-Rushing 2010; Vasconcellos et al. 2011; Huntly et al. 2021; Joseph and Kumar 2021; Pokorný 2021). The regularity of these environmental periodicities allows for species to adapt and respond to them (Bernhardt et al. 2020; Fretwell 1972; Shuter et al. 2012; Tonkin et al. 2017), meaning that nature has evolved around, and within, these complex temporal abiotic signatures (Mathias and Chesson 2013; Varpe 2017; Rudolf 2019). Despite the long-known recognition of nature's complex abiotic palette (White and Hastings 2020), relatively little ecological research has considered the scope of nature's abiotic variability in maintaining species diversity.

Researchers have cogently argued that temporal variations can promote species coexistence via fluctuation-dependent coexistence mechanisms (e.g., storage effect, relative nonlinearity, equalizing mechanisms) (Namba and Takahashi 1993; Chesson and Huntly 1997; Adler et al. 2006; Li and Chesson 2016; Miller and Klausmeier 2017; Chesson 2018; Johnson and Hastings 2022a, 2022b; Meyer et al. 2022). With these mechanisms, temporal niche differentiation enables coexistence between species with different competitive advantages that would otherwise not be possible in static

environments (Chesson 2000; Chan et al. 2009; Mathias and Chesson 2013; Scranton and Vasseur 2016; Miller and Klausmeier 2017; Rossi et al. 2017; Zielinski et al. 2017). For example, temporally changing resource conditions, which fluctuate between periods of high productivity to periods of very little to no productivity (Fretwell 1972; Campbell et al. 2008; Suski and Ridgway 2009; Huntly et al. 2021), may favour different species at different times (Armstrong and McGehee 1980; Litchman and Klausmeier 2001; Hastings 2012; Huntly et al. 2021). Even though species have developed biological responses to predict the timing of these changing conditions, the influence of abiotic periods on the ecology of species interactions is still in its infancy.

While competition theory has largely focussed on the mechanisms of species coexistence in non-periodic environments (e.g., predator-prey competition dynamics (Armstrong and McGehee 1976; Chen et al. 2013); invasion criteria (Kang and Chesson 2010; Mathias and Chesson 2013; Chesson 2018)), studies are beginning to suggest that periodic environments may have significant implications for species coexistence (Klausmeier 2010; Mathias and Chesson 2013; Chesson 2018; White and Hastings 2020). For example, the research by McMeans et al. (2020), illustrates how annual seasonal trade-offs promote species coexistence by allowing species to thrive during different seasons of the year. Another paper, by Mougi (2020), shows that the coupling of differently timed resource fluctuations (i.e., polyrhythms) may broaden the range of coexistence between diverse species that rely on limited resources. While these recent papers highlight the importance of temporal variations, the demand for a more general

theoretical understanding on the role of periodic conditions – either in isolation or as suites of periodicities (i.e., polyrhythms) – remains (White and Hastings 2020).

The fact that little research has been explored pertaining to the significance of these natural periodicities becomes critical as climate change is currently altering the nature of these environmental fluctuations (Dijkstra et al 2011; Shuter et al. 2012; Urban et al. 2012; Chesson 2018; Al-Habahbeh et al. 2020). Northern-hemisphere winters are becoming shorter in length and more moderate (Caldwell et al. 2020; Edlund et al. 2017; Ficker et al. 2017; Warne et al. 2020), and weather patterns across the globe are becoming more variable and unpredictable (Fang and Stefan 1998; O'Reilly et al. 2015). In response, many communities have experienced an increase in species extinction (Urban et al. 2012; Moor 2017; Fung et al. 2020) and invasion rates (Stachowicz et al. 2002; Sharma et al. 2009; Dijkstra et al. 2011; Cerasoli et al. 2019; Atkinson et al. 2020). Therefore, as climate change continues to alter the abiotic conditions to which organisms have adapted to, the mechanisms regulating species coexistence may be fundamentally altered (di Paola et al. 2012; Korpela et al. 2013; Tunney et al. 2014; Anderson et al. 2015; Eloranta et al. 2016; Bartley et al. 2019; Caldwell et al. 2020). With all this in mind, developing an understanding for the mechanisms behind the maintenance of biodiversity in periodic environments becomes even more crucial.

Here, we extend upon the seasonal coexistence model first introduced by McMeans et al. (2020), viewing it not only as an annual seasonal forcing model, but also as one that more generally considers the role of periodic forcing across all temporal lengths (e.g.,

days to multi-decadal) via different biological parameter combinations. As periodic environments may play a major role in species coexistence, we seek to generally explore which competitive outcomes may occur in these environments and under what biological conditions (i.e., different growth rates). Towards this, we employ an analytical approach consistent with the classical Lotka-Volterra phaseplane theory by developing a simple approximation that allows us to solve for the isocline solutions of a time-separated periodic model. Specifically, this approximation allows us to define coexistence criteria for periodic environments. We then illustrate how environmental periodicities can, in and of themselves, drive bifurcations (i.e., changing invasion criteria) that mediate coexistence, competitive exclusion, and contingent coexistence. We end by discussing our competition results in light of how climate change is altering the nature of key underlying abiotic periodicities.

Methods

We start by extending upon McMeans et al. (2020)'s annual seasonal model here, but more generally, we define a "season" as a discrete division in time that repeats itself, or is periodic, of any given length. As such, summer (more productive) and winter (less productive) seasons in McMeans et al. (2020) repeat themselves with a periodicity of one-year but we may also similarly decompose other natural shorter (e.g., seconds (Huntly et al. 2021)) and longer (e.g., El-Nino Southern Oscillations (Joseph and Kumar 2021)) periodicities into discrete seasons of more or less productive conditions. Towards this general understanding of periodicities, we extend the Lotka-Volterra competition model (Lotka 1920; Volterra 1928) into a periodic model that repeatedly

alternates between two discrete seasons, a productive (f_P) and less productive (f_{LP}) season. For each species, these functions are modelled with environmentally specific parameter combinations to incorporate biological constraints within each season, discussed below (Figure 1a). The Lotka-Volterra model is defined as:

$$f_{S,j}(t) = r_{S,j}X_j(1 - \alpha_{S,jj}X_j - \alpha_{S,jk}X_k) \quad (1)$$

where *j* and *k* represent two competing species, and *S* represents a season (either productive, *P*, or less productive, *LP*). Here, $r_{S,j}$ is the intrinsic rate of population growth for species *j* in a season, *S*, $\alpha_{S,jj}$ is the intraspecific competitive coefficient for species *j* in season *S*, and $\alpha_{S,jk}$ is the interspecific competitive coefficient for species *k* on species *j* in season *S*.

When running simulations, and to maintain the spirit of the model assumptions (i.e., productive and less productive season), we assumed the following simple biologically realistic assumptions:

(1) Maximal growth rates are larger in the productive period than the less productive period for both species (i.e., $r_{P,j} > r_{LP,j}$), and;

(2) Since resources are more available in the productive period compared to the less productive period, intraspecific competition will be lower in the productive period compared to the less productive period (i.e., $\alpha_{P,jj} < \alpha_{LP,jj}$).

Further, to incorporate realistic biological trade-offs between competing species, we assumed that species 1 is a better performer in the productive period compared to species 2, and the opposite is true in the less productive period. Keeping in mind the

previous seasonal constraints, this produces the following realistic parametric trade-offs for the two species:

(1) Species 1 has a higher growth rate in the productive period (i.e., $r_{P,1} > r_{P,2}$) and a lower growth rate in the less productive period (i.e., $r_{LP,2} > r_{LP,1}$) compared to species 2, and;

(2) Species 1 has a smaller intraspecific competitive coefficient in the productive period (i.e., $\alpha_{P,11} < \alpha_{P,22}$) and a larger intraspecific competitive coefficient in the less productive period (i.e., $\alpha_{LP,11} > \alpha_{LP,22}$) compared to species 2.

These trade-offs are similar to an empirical case study by McMeans et al. (2020) where cold-adapted fish (e.g., lake trout, *Salvelinus namaycush*) are seasonal generalists with moderate growth rates year-round, and warm-adapted fish (e.g., smallmouth bass, *Micropterus dolomieu*), the lake trout's competitor, are seasonal specialists with higher growth rates during the summer and lower growth rates during the winter.

With the above assumptions taken into consideration, our model is a periodic step function (repeats every 1-time unit), that goes through a productive time period (*P*), and a less productive time period (*LP*), as follows:

$$\frac{dX_j}{dt} = \begin{cases} f_{P,j}(t) & i < t < i + p \\ f_{LP,j}(t) & i + p < t < i + 1 \end{cases} \qquad (2)$$

where *i* = 0 to t_{END} = length of the model run, with an integer step size 1; *p* is the length of the productive interval as a proportion of each time unit (leaving (*1-p*) as the less productive interval); and *j* represents one of the two competitive species, either species 1 or 2. These periodic functions of f_P and f_{LP} are defined in equation (1) as f_S. Note,

that the model as framed does not define the time units on purpose. In this sense, here we seek general results that allow us to see how periodicity, of any length, may influence coexistence. As an example, if the units are in days, the above model would represent a one-day period (e.g., diurnal fluctuations), if the units were in years, the model would represent an annual period or seasonal period as in McMeans et al. (2020), and so on. Further, we note that once the time units are defined, biological rates scale accordingly which influences the parameter estimates of both the growth rates, *r*, and the competitive coefficients, α – inter- and intraspecific. For example, a small mammal with an instantaneous per capita growth rate of 2 on a scale of years (time units year^{-1}) will have a significantly higher growth rate on a timescale of 10 years and a much smaller growth rate on a timescale of 1 month. The size of the competitive coefficients, α, will also be altered by the timescales in a similar manner. In what follows, we find results that occur across broad swaths of *r* and α values suggesting that our results likely hold for a broad range of natural periodicities (e.g., days to multi-decadal), consistent with a recent analysis by Mougi (2020) which argued that scales of months to years ought to significantly aid species coexistence.

We coded all numerical simulations in Mathematica 12.0. The models are integrated over numerous years until an asymptotic state, referred to as an equilibrium state despite within-year variation has been reached (i.e., mean value from 900 – 1000 time-steps) to remove transient influences. However, within each time unit, as discussed above, they sequentially follow first productive then less productive parameters corresponding to the given productive seasonal fraction, *p*, within the year. The

productive seasonal fraction, *p*, allows us to change the proportion of the year that is under our productive conditions versus our less productive conditions, (1-*p*) (e.g., increase f_P) (Figure 1b).

Finally, all model parameterizations for our simulations can be found in our figure legends and in the supplement. Below we first walk through our approximation and then our general analytical results before using these biologically realistic constraints to show that our simulations match our analytical results. For each outcome, we explore how changing the periodic lengths, *p*, influences competitive coexistence and exclusion (Figure 1b; Table 1).

Results

Here, we present our approximated isocline solutions and investigate the resulting coexistence criteria and behaviour under seasonality. Next, we reveal that changing seasonal length, *p*, in response to climate change, mediates coexistence, competitive exclusion, and contingent coexistence. Finally, we explore the robustness of our seasonally-mediated outcomes with 2-parameter bifurcation diagrams using seasonal length and different growth rates as parametric values.

Approximate Isocline Solutions for the Periodic Lotka-Volterra Model

Although we use a periodically forced system, we can use equilibrium concepts to understand the dynamics of our model. Specifically, our model reaches an attractor such that the densities fluctuate modestly up and down on a timescale of 1-unit (i.e., the

periodicity) around a mean that does not change (i.e., an asymptotic state or dynamic equilibrium). Given this equilibrium-like dynamic, we are interested in considering this asymptotic behaviour in a manner similar to the way we would for a system that reaches a true equilibrium. Here, we provide an approximation for our model isoclines and equilibria that mirror those of the original Lotka-Volterra competition model.

Note that the isoclines can be solved by recognizing that each integer step of 1-time unit would necessarily have to result in a zero net growth (i.e., no overall changes in density between time steps, as in a classical Lotka-Volterra zero-growth isocline). That is, from System (2), the X_j zero-net-growth condition occurs when:

$$\frac{dX_j}{dt} = \begin{cases} f_{P,j}(t) & i < t < i + p \\ f_{LP,j}(t) & i + p < t < i + 1 \end{cases} = 0 \qquad (3)$$

Biologically, this occurs when the dynamics of X_j over the productive period (i.e., the population dynamics driven by $f_{P,j}(t)$) over the time interval *i* to *i+p* are identically negated by the change over the less productive period from *i+p* to *i+1* (i.e., the population dynamics driven by $f_{LP,j}(t)$). This logic holds for both species, and we can therefore solve for both the X_1 and X_2 zero-growth isocline solutions accordingly. In other words, this approach means that given any X_1-X_2 points on the phaseplane, then this X_1-X_2 point will be on one of the isoclines when System (3) is satisfied for a given species. Additionally, an X_1-X_2 point will be at an equilibrium when System (3) is satisfied for both species.

From System (3), the isocline solution follows as:

$$f_{P,j}(t)\Big|_{0}^{p} = f_{LP,j}(t)\Big|_{p}^{1} \tag{4}$$

This isocline solution (4) is not analytically tractable (note that each season has dynamics over a time interval), making it seem as though an isocline approach appears infeasible.

Towards solving for an approximate isocline, we note that for System (2), any X_1-X_2 co-ordinate at time *i* is on the isocline if at time *i+1* it is back at the same X_1-X_2 co-ordinate. Thus, the average of both trajectories – the productive trajectory over *p* followed by the less productive trajectory over (*1-p*) – accurately estimates the actual dynamics. For simplicity, by assuming that the instantaneous growth rates are linear, we approximate the productive trajectory over the time period, *p*, and solve the equations using the Fundamental Theorem of Calculus over the interval of a single time unit (see Supplementary Material S1) such that over the interval fraction, *p*, the productive trajectory necessarily scales linearly as:

$$\frac{dX_j}{dt} = pf_{P,j}(X_j, X_k) \tag{5}$$

and the less productive trajectory over the interval fraction (*1-p*) scales linearly as:

$$\frac{dX_j}{dt} = (1-p)f_{LP,j}(X_j, X_k) \tag{6}$$

Here, for simplicity, we first ignore the movement of the solution off the initial value over the interval *p*. Thus, both approximations (i.e., the productive (5) and less productive period (6)) operate on the same X_1-X_2 co-ordinate.

Given Equations (5) and (6), then the X_j-isocline occurs when:

$$pf_{P,j}\left(X_j, X_k\right) = -(1-p)f_{LP,j}(X_j, X_k) \tag{7}$$

This approximation (Equation (7)), if it works, can be solved symbolically as done elegantly for the classical Lotka-Volterra model and thus, such an approximation allows an entry point into well-known coexistence analyses and interpretations.

Substituting the productive and less productive models of Equation (1) for either species into Equation (7), the resulting isocline solutions, for both species, follow the following form:

$$X_j = \frac{pr_{P,j}\alpha_{P,jk} - (1-p)r_{LP,j}\alpha_{LP,jk}}{pr_{P,j}\alpha_{P,jj} - (1-p)r_{LP,j}\alpha_{LP,jj}} X_k + \frac{pr_{P,j} + (1-p)r_{LP,j}}{pr_{P,j}\alpha_{P,jj} - (1-p)r_{LP,j}\alpha_{LP,jj}} \tag{8}$$

The geometry of the approximated isoclines (Equation (8)) resembles that of the original Lotka-Volterra isoclines, which therefore allows us to identify general rules for coexistence in periodic environments akin to the original coexistence criteria (Figure 2a). Here, the isocline approximation solutions (and therefore coexistence criteria) are now based on temporal-growth-scaled inter- versus intra-specific competition rates (whereas the original Lotka-Volterra conditions are not dependent on growth rates; see Table 1 for Lotka-Volterra vs. Seasonal Coexistence Criteria). Thus, the approximation enables us to generally determine and graphically explore how periodicities and biological rates may interact in regulating competitive outcomes (Figure 2b). Immediately, based on these conditions, we can see that the duration of each season, and the corresponding biological conditions within them, play a critical role in regulating competitive outcomes in periodic environments. That is, our parameter *p* may drive

bifurcations, and therefore alter competitive outcomes under changing climatic conditions (Figure 2b).

We found numerically that this approximation works extraordinarily well (see Supplementary Material S2 for examples) and was, for example, able to repeatedly and accurately calculate the transcritical bifurcation points where an interior equilibrium intersects and exchanges stability, with an axial solution. Other approaches similar to our approximation, such as Klausmeier (2010)'s successional state dynamics, have been used to accurately investigate species coexistence when organismal dynamics are fast relative to their forcing speed. Given our assumption of linearity, the relative time scale of forcing vs. dynamics ought to be important for our approximation's accuracy. Indeed, when the dynamics become nonlinear with incredibly large growth rates, the approximation may fail to accurately match numerical simulations (see Supplementary Material S5), however the range at which this approximation holds is impressively robust.

General outcomes of changing environments

Given that changing seasonal lengths may have powerful implications for species coexistence, we now ask how changing seasonal length, p, (i.e., altering seasonal asymmetry) affects competitive outcomes. To do this we vary the seasonal length from p=0 (i.e., all less productive) to p=1 (i.e., all productive). We note that these endpoints are constant (i.e., no seasonality) and thus reduce to the classic Lotka-Volterra conditions based on the individual biological conditions for *P* or *LP* (Table 1).

Since McMeans et al. (2020) found the intriguing case of seasonally-mediated coexistence, we were interested in using our analytical results to unpack other examples of how seasonal change could fundamentally alter competitive outcomes. McMeans et al. (2020) noted that where the boundary conditions yielded competitive exclusion (i.e., exclusion at p=0 and p=1), a seasonal model could produce coexistence for intermediate p-values. This is intriguing as it immediately suggests that alterations in p (say from climate change) can drive exclusion. Importantly, our analytical solutions (Table 1) suggest that seasonality can mediate all possible competitive outcomes at intermediate p-values (Figure 3). Indeed, we found seasonally-mediated coexistence, competitive exclusion, and contingent coexistence (i.e., alternative states) (Figure 3a-c respectively).

For these seasonally-mediated outcomes, when the qualitative competitive outcome at intermediate p is fundamentally different from the extremes (i.e., p = 0 and 1), p drives a series of transcritical bifurcations that move the system between different conditions in Table 1 (shifts between shaded and clear zones indicate transcritical bifurcations that alter the qualitative nature of the attractor in Figure 3). Specifically, changing p always drives a series of two bifurcations for these seasonally-mediated outcomes (Figure 3). Other seasonally sensitive outcomes of course also result in p-driven bifurcations as seasonal patterns transition between the two endpoint conditions. Additionally, we note that these transcritical bifurcations can be considered as changes in the invasion criteria – in this case, seasonally-altered invasion criterion – as they are commonly referred to

in competition theory. For example, in Figure 3a, the gray shaded regions indicate that one species cannot invade from small densities while in the white or unshaded zone, it suddenly can invade from small densities.

Finally, clearly not all parameter combinations are sensitive to *p*-driven bifurcations. In these cases, *p* may simply drive changes in species' densities rather than shifts in the equilibrium structure (e.g., as seen in McMeans et al. (2020)). While here we broadly unpack *p*-driven bifurcations to explore the generality of these outcomes, we note that all results below have nearby solutions that are qualitatively continuous.

Robustness of Seasonally-Mediated Competitive Outcomes

To fully understand how robust the different seasonally-mediated outcomes are we looked at the bifurcation structure in 2-dimensional parameter space, by using both seasonal length, *p*, (as in Figure 3) and different growth rates, $r_{S,j}$, as bifurcation parameters. As discussed above, we note that if seasonally-mediated outcomes exist across a broad range of growth rate values, *r*, then this suggests that seasonally-mediated competitive outcomes may occur for both a range of natural periodicities and organismal life histories. Indeed, in all cases, we find that these different seasonally-mediated outcomes are quite general as the outcomes are found across a wide range of species' growth rates (Figures 4-6, S3.1.1, S3.2.1, S3.3.1). Here, we demonstrate the generality of these results using a single growth rate value (i.e., for one species in one season), but see Figure S3 for additional parameter ranges. Note that, to explore the

bifurcation structure generally for each parameter, some of our initial biological constraints have been relaxed.

In Figure 4a, we document cases where a lack of periodicity (i.e., at *p*=0 or 1) drives competitive exclusion while for a broad range of *r*'s (in this case, $r_{P,1}$), we have species coexistence at intermediate *p*-values. Our analytical solutions allow us to track the "mean equilibrium" through each transcritical bifurcation from competitive exclusion of species 1 to species coexistence and finally to competitive exclusion of species 2 as the length of the productive period, *p*, increases (Figures 4bi-iii, S4.1). The robustness of this pattern implies that for any given *r*, periodicity alone can mediate coexistence at intermediate seasonality (i.e., changing *p* moves from competitive exclusion to stable coexistence conditions in Table 1). As $r_{P,1}$ grows, this coexistence region travels from occurring at high *p*-values to low *p*-values, suggesting that the bifurcation structure may be sensitive to species' growth rates (which is also suggested by the seasonal coexistence criteria shown in Table 1), but the result is nonetheless general. This result is also seen across all other growth rates for each species in both productivity periods for seasonally-mediated coexistence (Figure S3.1.1). Thus, we see that seasonally-mediated coexistence occurs very broadly suggesting that periods of high and low productivity may be powerful drivers of coexistence.

Similarly, in Figure 5a, we document cases where species coexistence occurs in static environments (i.e., at *p*=0 or 1), while competitive exclusion occurs at intermediate *p*-values over a broad range of *r*'s (here, $r_{P,1}$). Following McMeans et al. (2020)'s naming

convention, we refer to this as seasonally-mediated competitive exclusion. As in the above case, with increasing *p*, our analytical approximation tracks the isoclines and the "mean equilibrium" from stable coexistence, to competitive exclusion of species 2 through a transcritical bifurcation on the X_2=0 axis, and finally back through the axis (via another bifurcation) to stable coexistence (Figures 5b, S4.2). The 2-dimensional parameter sensitivity analysis again shows a broad range in *r*-values that yield competitive exclusion; however, it does not stretch across all *r*-values (i.e., small *r*'s). While the exact range of parameter space that this seasonally-mediated competitive exclusion occurs at is clearly dependent on other parameters (including the $r_{P,1}$ value at which it manifests), this result is still quite general over a wide range of *r*-values, suggesting that periodicities may also be powerful drivers of competitive exclusion. Here, as $r_{P,1}$ grows, this tongue of competitive exclusion widens across intermediate values of *p*. This seasonally-mediated outcome can be found across all other growth rate values (Figure S3.2.1). Again, this is an interesting result suggesting that simple alterations in seasonal length may fundamentally alter competitive outcomes.

Finally, in Figure 6a, similar to the above seasonally-mediated coexistence case with competitive exclusion at the boundaries (i.e., *p*=0 or 1), we now document cases where contingent coexistence (i.e., alternative states) occurs at intermediate *p* values across a broad range of *r*'s (here, $r_{LP,2}$). Although this outcome is quite similar to seasonally-mediated coexistence as competitive exclusion is located at each boundary (i.e., *p*=0 or 1), its isocline geometry, based off of biological conditions, results in seasonally-mediated contingent coexistence at intermediate *p*-values (Figures 6bi-iii, S4.3). Our

approximation tracks the non-trivial (interior) equilibrium, which in this case is unstable while in positive (X_1, X_2) state space (Figure 6bii). Here initial densities determine which species will dominate and which species will become extinct with time (i.e., which of the two stable axial solutions, shown in Figure 6bii, the system will end up at; Namba and Takahashi 1993). The robustness of this pattern also implies that for a given *r*, periodicity may be a powerful driver of contingent coexistence (i.e., changing *p* moves from competitive exclusion to contingent coexistence conditions in Table 1). As $r_{LP,2}$ grows, this contingent coexistence region also moves from occurring at high *p*-values to low *p*-values. This result is found across all other growth rates for each species in both productivity periods for seasonally-mediated contingent coexistence (Figure S3.3.1).

These three seasonally-mediated outcomes suggest that seasonal alterations, due to climate change, may drive precipitous changes in competitive systems. All of these seasonally-mediated outcomes may be highly general and found across various ecosystems that experience periodic fluctuations. However, depending on parametric values, not all instances of periodic variation will drive these series of bifurcations. Under some conditions, there are simply *p*-driven changes in species densities between the boundary conditions where only one bifurcation (Figures S2.1e, S2.1f) or no bifurcation (Figure S2.1d) is found under changing periodicities.

Discussion

Here, we have used a simple linear approximation to analytically solve for a periodic Lotka-Volterra competition model (see Table 1 for seasonal coexistence criteria).

Importantly, this analytical approach produces approximate isoclines and equilibrium conditions that are remarkably similar to our numerical simulation results (e.g., predicts invasion criteria accurately; Figure S2.1). Akin to the longstanding classical Lotka-Volterra coexistence conditions, we derive a parallel set of coexistence conditions for periodic environments. With the inclusion of temporal periodicities, we find that species coexistence depends on seasonal-growth-scaled inter- versus intra-specific competition strengths (Table 1). That is, where classical stable coexistence requires intraspecific competition to be greater than interspecific competition, for both species, we show that intraspecific competition, scaled by seasonal growth, must be greater than interspecific competition, scaled by seasonal growth, for both species.

These seasonal coexistence conditions importantly suggest that species' coexistence may be incredibly sensitive to changes in seasonal length, seasonal growth rate trade-offs, and seasonal competitive trade-offs (both inter- and intraspecific). While McMeans et al. (2020) found seasonally-mediated coexistence through empirically-motivated numerical simulations, our results show that seasonality can mediate coexistence, competitive exclusion, and contingent coexistence (Figure 3). That is, seasonality, in and of itself, can drive all possible competitive outcomes (i.e., Table 1). As these seasonally-mediated outcomes appear across a vast range of species' per capita growth rates (Figures 4-6, S3.1.1, S3.2.1, S3.3.1) and inter- and intraspecific competitive coefficients (Figures S3.1.2, S3.2.2, S3.3.2), this suggests that these seasonally-mediated outcomes are quite robust. While not fully explored here, given that all competitive outcomes seem to occur for a majority of growth rates, it is plausible

that these outcomes occur across a wide range of environmental periodicities and life history strategies (i.e., fast vs. slow life history strategies).

Our seasonally-mediated outcomes suggest that species coexistence may be incredibly sensitive to changes in seasonal length, *p*, (Figure 3). Climate change is altering environmental periodicities across a range of temporal scales (Dijkstra et al. 2011; Shuter et al. 2012; Urban et al. 2012; Chesson 2018; Al-Habahbeh et al. 2020), and our results suggest that this could have sudden and drastic – sometimes unpredictable – effects on coexistence. Often the responses to changing periodicities are nonlinear, and some of these outcomes are unexpected based on the classical Lotka-Volterra conditions under non-seasonal environments (e.g., nonlinear paths between the boundary conditions at $p = 0$ and 1; Figures 3b, 5, S2.1b and d). As an example, we find cases where competitive exclusion occurs under intermediate periodicities, even though coexistence is expected under the same non-seasonal conditions (i.e., coexistence occurs for entirely low- or entirely high-productive conditions; Figure 3b). Alarmingly, these strong nonlinear effects of changing seasonal length, *p*, suggest that precipitous changes in species density and composition may unexpectedly occur as climate change alters the nature of seasonality.

Although simple, the McMeans et al. (2020)'s seasonal Lotka-Volterra competition model we examined here is based on biologically realistic assumptions about competitive species in seasonal environments. First, periodic environments are commonly reflected by times of high and low productivity, where species tend to flourish

during the productive periods, and decline (e.g., mortality-dominated) during the less productive periods as resource availability becomes sparse (Fretwell 1972; Litchman and Klausmeier 2001; Mutze 2009; Klausmeier 2010; Hastings 2012; Lyu et al. 2016; Vihtakari et al. 2016). These periodicities therefore impact species' growth rates, but also offer the potential for differential responses of competing species to seasonally-driven environmental variation (Chesson and Huntly 1997; Forrest and Miller-Rushing 2010; Shuter et al. 2012; Gao et al. 2016; Chesson 2018; Huang et al. 2019). It is well known that competing species can display temporal trade-offs in stochastic environments that can promote coexistence (Litchman and Klausmeier 2001; Angert et al. 2009; Klausmeier 2010; Shuter et al. 2012; Mougi 2020). For instance, Litchman and Klausmeier (2001) discovered that slow fluctuations in light promote stable coexistence between competing species of phytoplankton who exhibit temporal trade-offs in resource availability. More recently, and consistent with our theoretical results here, empirical evidence is beginning to suggest species may show trade-offs to regular periodic fluctuations that might promote coexistence. For example, a species may be a seasonal specialist (e.g., display a very high growth rate during one period and a low growth rate during the other period) while its competitor may be more of a temporal generalist, who's able to maintain roughly the same growth rate year-round (Niiyama 1990; Chan et al. 2009; Abrams et al. 2013; Korpela et al. 2013; Meyer et al. 2022).

While we concentrate on temporal forcing in our model, seasonal signals in competition may often be related to spatial-temporal and behavioural patterns that govern species' competitive outcomes (McMeans et al. 2020). As an example, in some cases, species

may migrate (Holt and Fryxell 2011; Teitelbaum et al. 2015; Tavecchia et al. 2016; le Corre et al. 2020; Moorter et al. 2021) or hibernate (Campbell et al. 2008; Giraldo-Perez et al. 2016) during less productive periods, opting out of competition when resources are scarce (Suski and Ridgway 2009). These behavioural strategies may counteract potential negative effects of periodic variation to some extent and thus promote coexistence by reducing competitive interactions during unfavourable times. More empirical research is needed to further understand these spatial and behavioural strategies, and seasonal trade-offs between competitive species, in order to understand their mechanistic role in maintaining biodiversity with climate change.

As nature abounds with temporal variations and periodicities, grasping a better understanding for coexistence mechanisms in these fluctuating environments is now even more crucial with climate change. We have provided an analytical solution to begin understanding these effects. Our research has uncovered three competitive outcomes that could be found across all periodic environments. As species coexistence appears to be incredibly sensitive to periodic variation, climate change has the potential to drastically impact future competitive outcomes in the natural world.

Acknowledgements

This research is funded by the University of Guelph’s Elgin Card Scholarship in Terrestrial Ecology. We would also like to thank Cortland K. Griswold for his comments and suggestions that helped improve this manuscript.

Code accessibility

All code to reproduce the above analyses and figures have been archived on Zenodo (version 1.0).

Literature Cited

Abrams, P. A., C. M. Tucker, and B. Gilbert. 2013. Evolution of the storage effect. Evolution 67(2):315–327. https://doi.org/10.1111/j.1558-5646.2012.01756.x

Adler, P. B., J. HilleRisLambers, P. C. Kyriakidis, Q. Guan, and J. M. Levine. 2006. Climate variability has a stabilizing effect on the coexistence of prairie grasses. Proceedings of the National Academy of Sciences of the United States of America 103(34):12793–12798. https://doi.org/10.1073/pnas.0600599103

Al-Habahbeh, A. K., S. Kortsch, B. A. Bluhm, F. Beuchel, B. Gulliksen, C. Ballantine, D. Cristini, and R. Primicerio. 2020. Arctic coastal benthos long-term responses to perturbations under climate warming. Philosophical Transactions. Series A, Mathematical, Physical, and Engineering Sciences 378(2181):20190355. https://doi.org/10.1098/rsta.2019.0355

Anderson, K. D., S. F. Heron, and M. S. Pratchett. 2015. Species-specific declines in the linear extension of branching corals at a subtropical reef, Lord Howe Island. Coral Reefs 34(2):479–490. https://doi.org/10.1007/s00338-014-1251-1

Angert, A. L., T. E. Huxman, P. Chesson, and D. L. Venable. 2009. Functional tradeoffs determine species coexistence via the storage effect. Proceedings of the National Academy of Sciences of the United States of America 106(28):11641–11645. https://doi.org/10.1073/pnas.0904512106

Armstrong, R. A., and R. McGehee. 1976. Coexistence of two competitors on one resource. Journal of Theoretical Biology 56(2):499–502. https://doi.org/10.1016/S0022-5193(76)80089-6

Armstrong, R. A., and R. McGehee. 1980. Competitive Exclusion. American Society of Naturalist 115(2):151–170.

Atkinson, J., N. G. King, S. B. Wilmes, and P. J. Moore. 2020. Summer and winter marine heatwaves favor an invasive over native seaweeds. Journal of Phycology 56(6):1591–1600. https://doi.org/10.1111/jpy.13051

Bartley, T. J., K. S. McCann, C. Bieg, K. Cazelles, M. Granados, M. M. Guzzo, A. S. MacDougall, T. D. Tunney, and B. C. McMeans. 2019. Food web rewiring in a changing world. Nature Ecology and Evolution 3(3):345–354. https://doi.org/10.1038/s41559-018-0772-3

Bernhardt, J., M. O'Connor, J. Sunday, and A. Gonzalez. 2020. Life in fluctuating environments. Philosophical Transactions of the Royal Society of London. Series B. Biological Sciences 375(1814):1–22. https://doi.org/10.32942/osf.io/dgmr4

Caldwell, T. J., S. Chandra, K. Feher, J. B. Simmons, and Z. Hogan. 2020. Ecosystem response to earlier ice break-up date: Climate-driven changes to water temperature, lake-habitat-specific production, and trout habitat and resource use. Global Change Biology 26(10):5475–5491. https://doi.org/10.1111/gcb.15258

Campbell, H. A., K. P. P. Fraser, C. M. Bishop, L. S. Peck, and S. Egginton. 2008. Hibernation in an Antarctic fish: On ice for winter. PLoS ONE 3(3). https://doi.org/10.1371/journal.pone.0001743

Cerasoli, F., M. Iannella, and M. Biondi. 2019. Between the hammer and the anvil: How the combined effect of global warming and the non-native common slider could threaten the european pond turtle. Management of Biological Invasions 10(3):428–448. https://doi.org/10.3391/mbi.2019.10.3.02

Chan, B., R. Durrett, and N. Lanchier. 2009. Coexistence for a multitype contact process with seasons. Annals of Applied Probability 19(5):1921–1943. https://doi.org/10.1214/09-AAP599

Chen, L., F. Chen, and Y. Wang. 2013. Influence of predator mutual interference and prey refuge on Lotka-Volterra predator-prey dynamics. Communications in Nonlinear Science and Numerical Simulation 18(11):3174–3180. https://doi.org/10.1016/j.cnsns.2013.04.004

Chesson, P. 2000. Mechanisms of maintenance of species diversity. Annual Review of Ecology and Systematics 31:343–366. https://doi.org/10.1146/annurev.ecolsys.31.1.343

Chesson, P. 2018. Updates on mechanisms of maintenance of species diversity. Journal of Ecology 106(5):1773–1794. https://doi.org/10.1111/1365-2745.13035

Chesson, P., and N. Huntly. 1997. The roles of harsh and fluctuating conditions in the dynamics of ecological communities. The American Naturalist 150(5):519–553.

di Paola, A., R. Valentini, and F. Paparella. 2012. Climate change threatens coexistence within communities of mediterranean forested wetlands. PLoS ONE *7*(10). https://doi.org/10.1371/journal.pone.0044727

Dijkstra, J. A., E. L. Westerman, and L. G. Harris. 2011. The effects of climate change on species composition, succession and phenology: A case study. Global Change Biology 17(7):2360–2369. https://doi.org/10.1111/j.1365-2486.2010.02371.x

Edlund, M. B., J. E. Almendinger, X. Fang, J. M. R. Hobbs, D. D. VanderMeulen, R. L. Key, and D. R. Engstrom. 2017. Effects of climate change on lake thermal structure and biotic response in northern wilderness lakes. Water 9(678):1-35. https://doi.org/10.3390/w9090678

Eloranta, A. P., I. P. Helland, O. T. Sandlund, T. Hesthagen, O. Ugedal, and A. G. Finstad. 2016. Community structure influences species' abundance along environmental gradients. Journal of Animal Ecology 85:273–282. https://doi.org/10.1111/1365-2656.12461

Fang, X., and H. G. Stefan. 1998. Potential climate warming effects on ice covers of small lakes in the contiguous U.S. Cold Regions Science and Technology 27(2):119–140. https://doi.org/10.1016/S0165-232X(97)00027-X

Ficker, H., M. Luger, and H. Gassner. 2017. From dimictic to monomictic: Empirical evidence of thermal regime transitions in three deep alpine lakes in Austria induced by climate change. Freshwater Biology 62(8):1335–1345. https://doi.org/10.1111/fwb.12946

Forrest, J., and A. J. Miller-Rushing. 2010. Toward a synthetic understanding of the role of phenology in ecology and evolution. Philosophical Transactions of the Royal Society B: Biological Sciences 365(1555):3101–3112. https://doi.org/10.1098/rstb.2010.0145

Fretwell, S. D. 1972. Populations in a seasonal environment. Princeton University Press.

Fung, T., R. A. Chisholm, K. Anderson-Teixeira, N. Bourg, W. Y. Brockelman, S. Bunyavejchewin, C. H. Chang-Yang, R. Chitra-Tarak, G. Chuyong, R. Condit, H. S. Dattaraja, S. J. Davies, C. E. N. Ewango, G. Fewless, C. Fletcher, C. V. S. Gunatilleke, I. A. U. N. Gunatilleke, Z. Hao, J. A. Hogan, … J. Zimmerman. 2020. Temporal population variability in local forest communities has mixed effects on tree species richness across a latitudinal gradient. Ecology Letters *23*(1):160–171. https://doi.org/10.1111/ele.13412

Gao, G., S. Ponsard, Z. Lu, P. Wang, and S. Sharma. 2016. Different thermal responses in two coexisting aphids may account for differences in their seasonal abundance in cotton fields. International Journal of Pest Management *62*(4):288–294. https://doi.org/10.1080/09670874.2016.1185551

Giraldo-Perez, P., P. Herrera, A. Campbell, M. L. Taylor, A. Skeats, R. Aggio, N. Wedell, and T. A. R. Price. 2016. Winter is coming: Hibernation reverses the outcome of sperm competition in a fly. Journal of Evolutionary Biology 29(2):371–379. https://doi.org/10.1111/jeb.12792

Hastings, A. 2012. Temporally varying resources amplify the importance of resource input in ecological populations. Biology Letters 8(6):1067–1069. https://doi.org/10.1098/rsbl.2012.0669

Holt, R. D., and J. M. Fryxell. 2011. Theoretical reflections on the evolution of migration. Pages 17–31 *in* E. J. Milner-Gulland, J. M. Fryxell, and A. R. E. Sinclaire, eds. Animal migration. Oxford University Press, Oxford. https://doi.org/10.1093/acprof:oso/9780199568994.003.0003

Huang, L., W. Xue, and T. Herben. 2019. Temporal niche differentiation among species changes with habitat productivity and light conditions. Journal of Vegetation Science 30(3):438–447. https://doi.org/10.1111/jvs.12741

Huntly, N., A. R. Freischel, A. K. Miller, M. C. Lloyd, D. Basanta, and J. S. Brown. 2021. Coexistence of “cream skimmer” and “crumb picker” phenotypes in nature and in cancer. Frontiers in Ecology and Evolution 9:1–18. https://doi.org/10.3389/fevo.2021.697618

Jackson, M. C., S. Pawar, and G. Woodward. 2021. The temporal dynamics of multiple stressor effects: From individuals to ecosystems. Trends in Ecology and Evolution 36(5):402–410. https://doi.org/10.1016/j.tree.2021.01.005

Jiang, L., and P. J. Morin. 2007. Temperature fluctuation facilitates coexistence of competing species in experimental microbial communities. Journal of Animal Ecology 76(4):660–668. https://doi.org/10.1111/j.1365-2656.2007.01252.x

Johnson, E., and A. Hastings. 2022a. Coexistence in spatiotemporally fluctuating environments. Research Square 1–67. https://doi.org/https://doi.org/10.21203/rs.3.rs-1308669/v1 License:

Johnson, E., and A. Hastings. 2022b. Towards a heuristic understanding of the storage effect. Ecology Letters 00:1–12. https://doi.org/10.1111/ele.14112

Joseph, D., and V. S. Kumar. 2021. Response of ocean surface waves to the co-occurrence of Boreal Summer Intra-Seasonal Oscillation and El Niño Southern Oscillation. Climate Dynamics 57(3–4) :1155–1171. https://doi.org/10.1007/s00382-021-05763-3

Kang, Y., and P. Chesson. 2010. Relative nonlinearity and permanence. Theoretical Population Biology 78(1):26–35. https://doi.org/10.1016/j.tpb.2010.04.002

Klausmeier, C. A. 2010. Successional state dynamics: A novel approach to modeling nonequilibrium foodweb dynamics. Journal of Theoretical Biology 262(4):584–595. https://doi.org/10.1016/j.jtbi.2009.10.018

Korpela, K., M. Delgado, H. Henttonen, E. Korpimäki, E. Koskela, O. Ovaskainen, H. Pietiäinen, J. Sundell, N. G. Yoccoz, and O. Huitu. 2013. Nonlinear effects of

climate on boreal rodent dynamics: Mild winters do not negate high-amplitude cycles. Global Change Biology 19(3):697–710. https://doi.org/10.1111/gcb.12099

le Corre, M., C. Dussault, and S. D. Côté. 2020. Where to spend the winter? The role of intraspecific competition and climate in determining the selection of wintering areas by migratory caribou. Oikos 129(4):512–525. https://doi.org/10.1111/oik.06668

Li, L., and P. Chesson. 2016. The effects of dynamical rates on species coexistence in a variable environment: The paradox of the plankton revisited. American Naturalist 188(2):E46–E58. https://doi.org/10.1086/687111

Litchman, E., and C. A. Klausmeier. 2001. Competition of phytoplankton under fluctuating light. American Naturalist 157(2):170–187. https://doi.org/10.1086/318628

Lotka, A. J. 1920. Analytical note on certain rhythmic relations in organic systems. Proceedings of the National Academy of Sciences of the United States of America 6(7):410–415.

Lyu, L., X. Deng, and Q. B. Zhang. 2016. Elevation pattern in growth coherency on the southeastern Tibetan Plateau. PLoS ONE 11(9):1–15. https://doi.org/10.1371/journal.pone.0163201

Mathias, A., and P. Chesson. 2013. Coexistence and evolutionary dynamics mediated by seasonal environmental variation in annual plant communities. Theoretical Population Biology 84(1):56–71. https://doi.org/10.1016/j.tpb.2012.11.009

McMeans, B. C., K. S. McCann, M. M. Guzzo, T. J. Bartley, C. Bieg, P. J. Blanchfield, T. Fernandes, H. C. Giacomini, T. Middel, M. D. Rennie, M. S. Ridgway, and B. J. Shuter. 2020. Winter in water: Differential responses and the maintenance of biodiversity. Ecology Letters 23(6):922–938. https://doi.org/10.1111/ele.13504

Meyer, I., B. Steinmetz, and N. M. Shnerb. 2022. How the storage effect and the number of temporal niches affect biodiversity in stochastic and seasonal environments. PLoS Computational Biology 18(3):1–21. https://doi.org/10.1371/journal.pcbi.1009971

Miller, E. T., and C. A. Klausmeier. 2017. Evolutionary stability of coexistence due to the storage effect in a two-season model. Theoretical Ecology 10(1):91–103. https://doi.org/10.1007/s12080-016-0314-z

Moor, H. 2017. Life history trade-off moderates model predictions of diversity loss from climate change. PLoS ONE 12(5):1–21. https://doi.org/10.1371/journal.pone.0177778

Moorter, B. V, N. J. Singh, C. M. Rolandsen, E. J. Solberg, H. Dettki, J. Pusenius, J. Månsson, H. Sand, J. M. Milner, O. Roer, A. Tallian, W. Neumann, G. Ericsson, and A. Mysterud. 2021. Seasonal release from competition explains partial migration in European moose. Oikos 130(9):1548–1561. https://doi.org/10.1111/oik.07875

Mougi, A. 2020. Polyrhythmic foraging and competitive coexistence. Scientific Reports 10(1):1–7. https://doi.org/10.1038/s41598-020-77483-3

Mutze, G. J. 2009. Changes in body condition and body size affect breeding and recruitment in fluctuating house mouse populations in south-eastern Australia. Austral Ecology 34(3):278–293. https://doi.org/10.1111/j.1442-9993.2008.01929.x

Namba, T., and S. Takahashi. 1993. Competitive coexistence in a seasonally fluctuating environment II. Multiple stable states and invasion success. Theoretical Population Biology 44(3):374–402. https://doi.org/10.1006/tpbi.1993.1033

Niiyama, K. 1990. The role of seed dispersal and seedling traits in colonization and coexistence of Salix species in a seasonally flooded habitat. Ecological Research 5:317–331.

O'Reilly, C. M., S. Sharma, D. K. Gray, S. E. Hampton, J. S. Read, R. J. Rowley, P. Schneider, J. D. Lenters, P. B. McIntyre, B. M. Kraemer, G. A. Weyhenmeyer, D. Straile, B. Dong, R. Adrian, M. G. Allan, O. Anneville, L. Arvola, J. Austin, J. L. Bailey, … G. Zhang. 2015. Rapid and highly variable warming of lake surface waters around the globe. Geophysical Research Letters 42(24):10773–10781. https://doi.org/10.1002/2015GL066235

Pokorný, V. 2021. Polyrhythmic arrangements: Rhythm as a dynamic principle in the constitution of environments. Open Philosophy 4(1):394–403. https://doi.org/10.1515/opphil-2020-0192

Rossi, V., A. Martorella, D. Scudieri, and P. Menozzi. 2017. Seasonal niche partitioning and coexistence of amphimictic and parthenogenetic lineages of Heterocypris

barbara (Crustacea: Ostracoda). Canadian Journal of Zoology 95(1):7–14. https://doi.org/10.1139/cjz-2016-0038

Rudolf, V. H. W. 2019. The role of seasonal timing and phenological shifts for species coexistence. Ecology Letters 22(8):1324–1338. https://doi.org/10.1111/ele.13277

Scranton, K., and D. A. Vasseur. 2016. Coexistence and emergent neutrality generate synchrony among competitors in fluctuating environments. Theoretical Ecology 9(3):353–363. https://doi.org/10.1007/s12080-016-0294-z

Sharma, S., D. A. Jackson, and C. K. Minns. 2009. Quantifying the potential effects of climate change and the invasion of smallmouth bass on native lake trout populations across Canadian lakes. Ecography 32(3):517–525. https://doi.org/10.1111/j.1600-0587.2008.05544.x

Shuter, B. J., A. G. Finstad, I. P. Helland, I. Zweimüller, and F. Hölker. 2012. The role of winter phenology in shaping the ecology of freshwater fish and their sensitivities to climate change. Aquatic Sciences 74(4):637–657. https://doi.org/10.1007/s00027-012-0274-3

Stachowicz, J. J., J. R. Terwin, R. B. Whitlatch, and R. W. Osman. 2002. Linking climate change and biological invasions: Ocean warming facilitates nonindigenous species invasions. Proceedings of the National Academy of Sciences of the United States of America 99(24):15497–15500. https://doi.org/10.1073/pnas.242437499

Suski, C. D., and M. S. Ridgway. 2009. Winter biology of centrarchid fishes. Pages 264–292 *in* S. J. Cooke and D. P. Philipp, eds. Centrarchid Fishes. Blackwell Publishing Ltd. https://doi.org/10.1002/9781444316032.ch9

Tavecchia, G., S. Tenan, R. Pradel, J. M. Igual, M. Genovart, and D. Oro. 2016. Climate-driven vital rates do not always mean climate-driven population. Global Change Biology 22(12):3960–3966. https://doi.org/10.1111/gcb.13330

Teitelbaum, C. S., W. F. Fagan, C. H. Fleming, G. Dressler, J. M. Calabrese, P. Leimgruber, and T. Mueller. 2015. How far to go? Determinants of migration distance in land mammals. Ecology Letters 18(6):545–552. https://doi.org/10.1111/ele.12435

Tonkin, J. D., M. T. Bogan, N. Bonada, B. Rios-Touma, and D. A. Lytle. 2017. Seasonality and predictability shape temporal species diversity. Ecology 98(5):1201–1216. https://doi.org/10.1002/ecy.1761

Tunney, T. D., K. S. McCann, N. P. Lester, and B. J. Shuter. 2014. Effects of differential habitat warming on complex communities. Proceedings of the National Academy of Sciences of the United States of America 111(22):8077–8082. https://doi.org/10.1073/pnas.1319618111

Urban, M. C., L. de Meester, M. Vellend, R. Stoks, and J. Vanoverbeke. 2012. A crucial step toward realism: Responses to climate change from an evolving metacommunity perspective. Evolutionary Applications 5(2):154–167. https://doi.org/10.1111/j.1752-4571.2011.00208.x

Varpe, Ø. 2017. Life history adaptations to seasonality. Integrative and Comparative Biology 57(5):943–960. https://doi.org/10.1093/icb/icx123

Vasconcellos, R. M., F. G. Araújo, J. N. de Sousa Santos, and M. de Araújo Silva. 2011. Diel seasonality in fish biodiversity in a sandy beach in south-eastern Brazil. Marine Biological Association of the United Kingdom 91(6):1337–1344. https://doi.org/10.1017/S0025315410000652

Vihtakari, M., P. E. Renaud, L. J. Clarke, M. J. Whitehouse, H. Hop, M. L. Carroll, and W. G. Ambrose. 2016. Decoding the oxygen isotope signal for seasonal growth patterns in Arctic bivalves. Palaeogeography, Palaeoclimatology, Palaeoecology 446:263–283. https://doi.org/10.1016/j.palaeo.2016.01.008

Volterra, V. 1928. Variations and fluctuations of the number of individuals in animal species living together. ICES Journal of Marine Science 3(1):3–51. https://doi.org/10.1093/icesjms/3.1.3

Warne, C. P. K., K. S. McCann, N. Rooney, K. Cazelles, and M. M. Guzzo. 2020. Geography and morphology affect the ice duration dynamics of northern hemisphere lakes worldwide. Geophysical Research Letters 47(12):1–10. https://doi.org/10.1029/2020GL087953

White, E. R., and A. Hastings. 2020. Seasonality in ecology: Progress and prospects in theory. Ecological Complexity 44(100867):1–6. https://doi.org/10.1016/j.ecocom.2020.100867

Zielinski, W. J., J. M. Tucker, and K. M. Rennie. 2017. Niche overlap of competing carnivores across climatic gradients and the conservation implications of climate change at geographic range margins. Biological Conservation 209:533–545. https://doi.org/10.1016/j.biocon.2017.03.016

Tables

Table 1: Lotka-Volterra Coexistence Conditions vs. Seasonal Coexistence Conditions.

	Lotka – Volterra Criteria	Seasonal Coexistence Criteria
Stable Coexistence	$\alpha_{11} > \alpha_{21}$	$\frac{\mathbf{pr_{P,1}\alpha_{P,11} + (1-p)r_{LP,1}\alpha_{LP,11}}}{\mathbf{pr_{P,1} + (1-p)r_{LP,1}}} > \frac{\mathbf{pr_{P,2}\alpha_{P,21} + (1-p)r_{LP,2}\alpha_{LP,21}}}{\mathbf{pr_{P,2} + (1-p)r_{LP,2}}}$
	$\alpha_{22} > \alpha_{12}$	$\frac{\mathbf{pr_{P,2}\alpha_{P,22} + (1-p)r_{LP,2}\alpha_{LP,22}}}{\mathbf{pr_{P,2} + (1-p)r_{LP,2}}} > \frac{\mathbf{pr_{P,1}\alpha_{P,12} + (1-p)r_{LP,1}\alpha_{LP,12}}}{\mathbf{pr_{P,1} + (1-p)r_{LP,1}}}$
Competitive Exclusion by sp_1	$\alpha_{11} > \alpha_{21}$	$\frac{\mathbf{pr_{P,1}\alpha_{P,11} + (1-p)r_{LP,1}\alpha_{LP,11}}}{\mathbf{pr_{P,1} + (1-p)r_{LP,1}}} > \frac{\mathbf{pr_{P,2}\alpha_{P,21} + (1-p)r_{LP,2}\alpha_{LP,21}}}{\mathbf{pr_{P,2} + (1-p)r_{LP,2}}}$
	$\alpha_{22} < \alpha_{12}$	$\frac{\mathbf{pr_{P,2}\alpha_{P,22} + (1-p)r_{LP,2}\alpha_{LP,22}}}{\mathbf{pr_{P,2} + (1-p)r_{LP,2}}} < \frac{\mathbf{pr_{P,1}\alpha_{P,12} + (1-p)r_{LP,1}\alpha_{LP,12}}}{\mathbf{pr_{P,1} + (1-p)r_{LP,1}}}$
Competitive Exclusion by sp_2	$\alpha_{11} > \alpha_{21}$	$\frac{\mathbf{pr_{P,1}\alpha_{P,11} + (1-p)r_{LP,1}\alpha_{LP,11}}}{\mathbf{pr_{P,1} + (1-p)r_{LP,1}}} > \frac{\mathbf{pr_{P,2}\alpha_{P,21} + (1-p)r_{LP,2}\alpha_{LP,21}}}{\mathbf{pr_{P,2} + (1-p)r_{LP,2}}}$
	$\alpha_{22} < \alpha_{12}$	$\frac{\mathbf{pr_{P,2}\alpha_{P,22} + (1-p)r_{LP,2}\alpha_{LP,22}}}{\mathbf{pr_{P,2} + (1-p)r_{LP,2}}} < \frac{\mathbf{pr_{P,1}\alpha_{P,12} + (1-p)r_{LP,1}\alpha_{LP,12}}}{\mathbf{pr_{P,1} + (1-p)r_{LP,1}}}$
Contingent Coexistence	$\alpha_{11} < \alpha_{21}$	$\frac{\mathbf{pr_{P,1}\alpha_{P,11} + (1-p)r_{LP,1}\alpha_{LP,11}}}{\mathbf{pr_{P,1} + (1-p)r_{LP,1}}} < \frac{\mathbf{pr_{P,2}\alpha_{P,21} + (1-p)r_{LP,2}\alpha_{LP,21}}}{\mathbf{pr_{P,2} + (1-p)r_{LP,2}}}$
	$\alpha_{22} < \alpha_{12}$	$\frac{\mathbf{pr_{P,2}\alpha_{P,22} + (1-p)r_{LP,2}\alpha_{LP,22}}}{\mathbf{pr_{P,2} + (1-p)r_{LP,2}}} < \frac{\mathbf{pr_{P,1}\alpha_{P,12} + (1-p)r_{LP,1}\alpha_{LP,12}}}{\mathbf{pr_{P,1} + (1-p)r_{LP,1}}}$

Figure Legends

Figure 1: Model schematic investigates the projected mean equilibrium density over the length of the productive period when species compete under different periodic conditions. a) The model set-up investigates two time-separated seasons with different environmental conditions (productive (white box) and less productive (gray box)). In numerical simulations, competitive species, X_1 (white fish) and X_2 (black fish), exhibit different trade-offs in response to these differing environmental conditions, where each species may experience different levels of inter- to intraspecific competitive interactions (thickness of arrows) depending on which species may have an overall better performance in one period compared to the other. An experiment is projected over an extensive amount of time (say 1000-time units) until it reaches an asymptotic state (we refer to this as an equilibrium despite the within-year variation). b) In the model experiment, the projected mean equilibrium density, which represents a fluctuating' species density at its asymptote, is calculated as the duration of the productive period (as a proportion of each time unit) varies from 0 – 1.

Figure 2: Isocline approximation of X_1 density on X_2 density. a) Stable coexistence isocline approximation on phaseplane of X_1 (dashed line) and X_2 (solid line) densities. Approximate isocline solutions for a given species occur when the instantaneous rate of change (represented by vector arrows) in each season, scaled by seasonal duration, are equal and opposite of each other (i.e., they “cancel” each other out such that the net change over a full period is null). Refer to Table 1 for similarities to Lotka–Volterra

coexistence conditions. b i-iii) illustrates a *p*-driven bifurcation, showing the movement of the isoclines as the productivity period travels from i) p = 0.5; coexistence, to ii) p = 0.6; transcritical bifurcation, to iii) p = 0.7; competitive exclusion. Parametric values: $\alpha_{P,11}$=0.44, $\alpha_{P,22}$=0.66, $\alpha_{P,12}$=0.25, $\alpha_{P,21}$=0.53, $\alpha_{LP,11}$=1.11, $\alpha_{LP,22}$=0.83, $\alpha_{LP,12}$=1.83, $\alpha_{LP,21}$=0.48, $r_{P,1}$=1.7, $r_{P,2}$=1.2, $r_{LP,1}$=0.3, $r_{LP,2}$=1.

Figure 3: Numerical simulations of mean density over length of productive period (p) for seasonally-mediated outcomes. White zone represents stable coexistence, light gray zone represents competitive exclusion, and dark gray zone represents contingent coexistence where the equilibrium is unstable and multiple attractors exist between the two species. a) Seasonally-mediated coexistence. Parametric values: $\alpha_{P,21}$=0.53, $\alpha_{P,12}$=0.25, $\alpha_{P,11}$=0.5, $\alpha_{P,22}$=0.66, $r_{P,1}$=1.7, $r_{P,2}$=1.2, $\alpha_{LP,21}$=0.583, $\alpha_{LP,12}$=1.22, $\alpha_{LP,11}$=1.11, $\alpha_{LP,22}$=0.83, $r_{LP,1}$=0.3, $r_{LP,2}$=1. b) Seasonally-mediated competitive exclusion. Parametric values: $\alpha_{P,21}$=0.4, $\alpha_{P,12}$=0.3125, $\alpha_{P,11}$=0.625, $\alpha_{P,22}$=0.66, $r_{P,1}$=4, $r_{P,2}$=1.2, $\alpha_{LP,21}$=1.14, $\alpha_{LP,12}$=0.8, $\alpha_{LP,11}$=2, $\alpha_{LP,22}$=1.43 $r_{LP,1}$=0.3, $r_{LP,2}$=1. c) Seasonally-mediated contingent coexistence. Parametric values; $\alpha_{P,21}$=0.83, $\alpha_{P,12}$=0.5, $\alpha_{P,11}$=0.5, $\alpha_{P,22}$=0.55, $r_{P,1}$=1.7, $r_{P,2}$=1.2, $\alpha_{LP,21}$=2, $\alpha_{LP,12}$=2.86, $\alpha_{LP,11}$=2.5, $\alpha_{LP,22}$=1, $r_{LP,1}$=0.3, $r_{LP,2}$=1.

Figure 4: Two-dimensional bifurcation diagram of seasonally-mediated coexistence**.** a) seasonally-mediated coexistence expanding over a wide range of possible growth rate values. Black arrow represents species 1's productive growth rate value ($r_{P,1}$=1.7) which tracks the numerical trajectory displayed in Figure 3a. Black dashes on this arrow indicate different qualitative competitive outcomes as changing p moves the isocline

approximation (in b)) from one competitive outcome to another. Half shaded, half open circles represent transcritical bifurcations at p=0.115 and p=0.69 (see Figure S4.1 for complete transition across p). b) isocline approximation tracks the approximate equilibrium, which represents the mean asymptotic behavior, as the productive season decreases from i) p=0.8; competitive exclusion, to ii) p=0.4; stable coexistence, to iii) p=0.1; competitive exclusion. Shaded circles are stable equilibrium points, and open circles are unstable equilibrium points. Parametric values: $\alpha_{P,21}$=0.53, $\alpha_{P,12}$=0.25, $\alpha_{P,11}$=0.5, $\alpha_{P,22}$=0.66, $r_{P,2}$=1.2, $\alpha_{LP,21}$=0.583, $\alpha_{LP,12}$=1.22, $\alpha_{LP,11}$=1.11, $\alpha_{LP,22}$=0.83, $r_{LP,1}$=0.3, $r_{LP,2}$=1.

Figure 5: Two-dimensional bifurcation diagram of seasonally-mediated competitive exclusion. a) seasonally-mediated competitive exclusion expanding over a wide range of possible growth rate values. Black arrow represents species 1's productive growth rate value ($r_{P,1}$=4) which tracks the numerical trajectory displayed in Figure 3b. Black dashes on this arrow indicate different qualitative competitive outcomes as changing p moves the isocline approximation (in b)) from one competitive outcome to another. Half shaded, half open circles represent transcritical bifurcations at p=0.17 and p=0.54 (see Figure S4.2 for complete transition across p). b) isocline approximation tracks the approximate equilibrium, which represents the mean asymptotic behaviour, as the productive season decreases from i) p=0.8; stable coexistence, to ii) p=0.4; competitive exclusion, to iii) p=0.1; stable coexistence. Shaded circles are stable equilibrium points, and open circles are unstable equilibrium points. Parametric values: $\alpha_{P,21}$=0.4,

$\alpha_{P,12}$=0.3125, $\alpha_{P,11}$=0.625, $\alpha_{P,22}$=0.66, $r_{P,2}$=1.2, $\alpha_{LP,21}$=1.14, $\alpha_{LP,12}$=0.8, $\alpha_{LP,11}$=2, $\alpha_{LP,22}$=1.43 $r_{LP,1}$=0.3, $r_{LP,2}$=1.

Figure 6: Two-dimensional bifurcation diagram of seasonally-mediated contingent coexistence. a) seasonally-mediated contingent coexistence expanding over a wide range of possible growth rate values. Black arrow represents species 2's less productive growth rate value ($r_{LP,2}$=1) which tracks the numerical trajectory displayed in Figure 3c. Black dashes on this arrow indicate different qualitative competitive outcomes as changing *p* moves the isocline approximation (in b)) from one competitive outcome to another. Half shaded, half open circles represent transcritical bifurcations at *p*=0.07 and *p*=0.69 (see Figure S4.3 for complete transition across *p*). b) isocline approximation isocline approximation tracks the approximate equilibrium, which represents the mean asymptotic behaviour, as the productive season decreases from i) *p*=0.8; competitive exclusion, to ii) *p*=0.4; contingent coexistence, to iii) *p*=0.0; competitive exclusion. Shaded circles are stable equilibrium points, and open circles are unstable equilibrium points. Parametric values; $\alpha_{P,21}$=0.83, $\alpha_{P,12}$=0.5, $\alpha_{P,11}$=0.5, $\alpha_{P,22}$=0.55, $r_{P,1}$=1.7, $r_{P,2}$=1.2, $\alpha_{LP,21}$=2, $\alpha_{LP,12}$=2.86, $\alpha_{LP,11}$=2.5, $\alpha_{LP,22}$=1, $r_{LP,1}$=0.3.

Figure 1

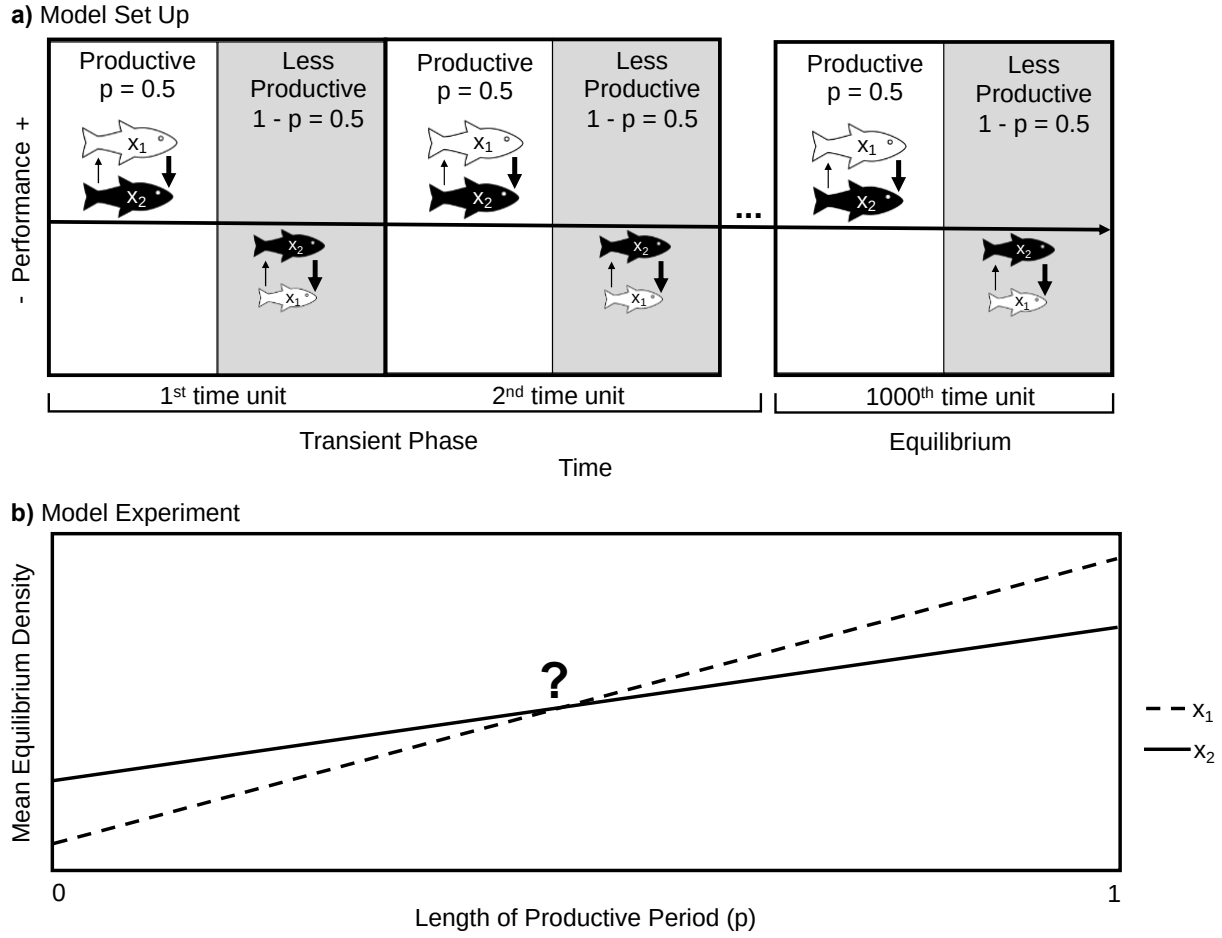
a) Model Set Up
Productive
p = 0.5
Less
Productive
1 - p = 0.5
Productive
p = 0.5
Less
Productive
1 - p = 0.5
Productive
p = 0.5
Less
Productive
1 - p = 0.5
x1
x2
...
- Performance +
1st time unit
2nd time unit
1000th time unit
Transient Phase
Equilibrium
Time
b) Model Experiment
Mean Equilibrium Density
?
x1
x2
0
1
Length of Productive Period (p)

Figure 2

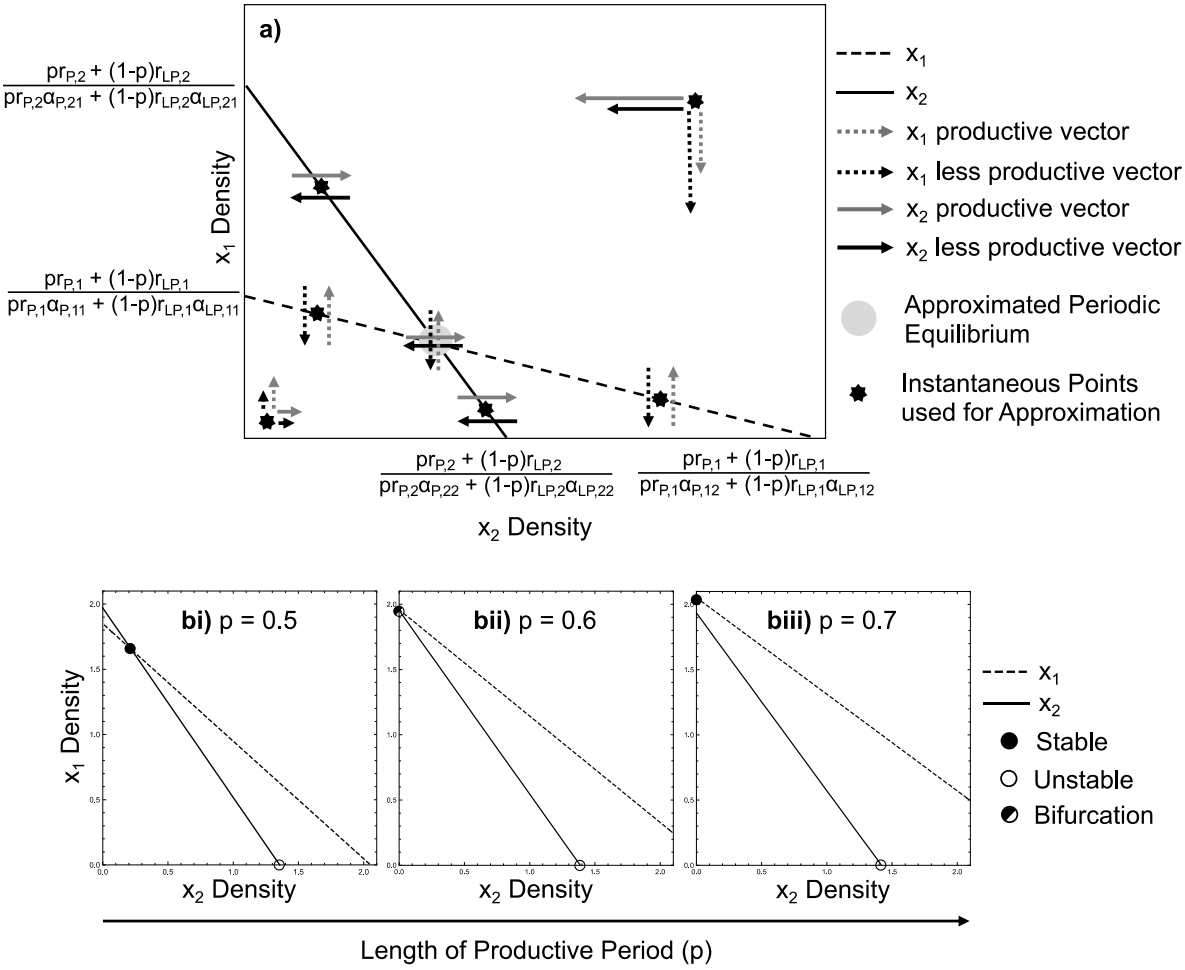
a)
$\frac{pr_{P,2} + (1-p)r_{LP,2}}{pr_{P,2}\alpha_{P,21} + (1-p)r_{LP,2}\alpha_{LP,21}}$
$\frac{pr_{P,1} + (1-p)r_{LP,1}}{pr_{P,1}\alpha_{P,11} + (1-p)r_{LP,1}\alpha_{LP,11}}$
x_1 Density
$\frac{pr_{P,2} + (1-p)r_{LP,2}}{pr_{P,2}\alpha_{P,22} + (1-p)r_{LP,2}\alpha_{LP,22}}$
$\frac{pr_{P,1} + (1-p)r_{LP,1}}{pr_{P,1}\alpha_{P,12} + (1-p)r_{LP,1}\alpha_{LP,12}}$
x_2 Density
x_1
x_2
x_1 productive vector
x_1 less productive vector
x_2 productive vector
x_2 less productive vector
Approximated Periodic Equilibrium
Instantaneous Points used for Approximation

bi) p = 0.5
bii) p = 0.6
biii) p = 0.7
x_1 Density
x_2 Density
x_1
x_2
Stable
Unstable
Bifurcation
Length of Productive Period (p)

Figure 3

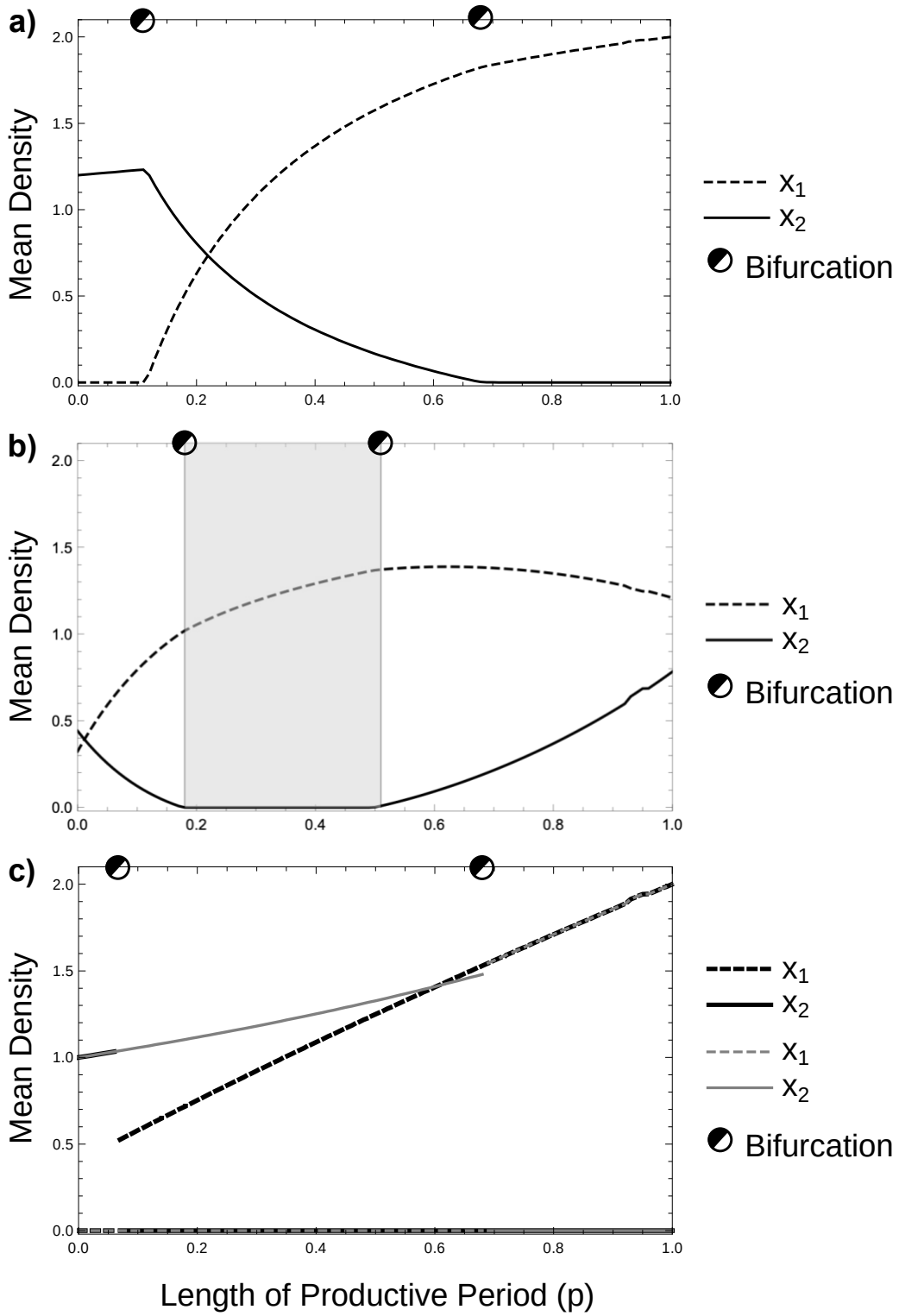
a)
b)
c)
Mean Density
Length of Productive Period (p)
0.0
0.5
1.0
1.5
2.0
0.0
0.2
0.4
0.6
0.8
1.0
x1
x2
x1
x2
Bifurcation

Figure 4

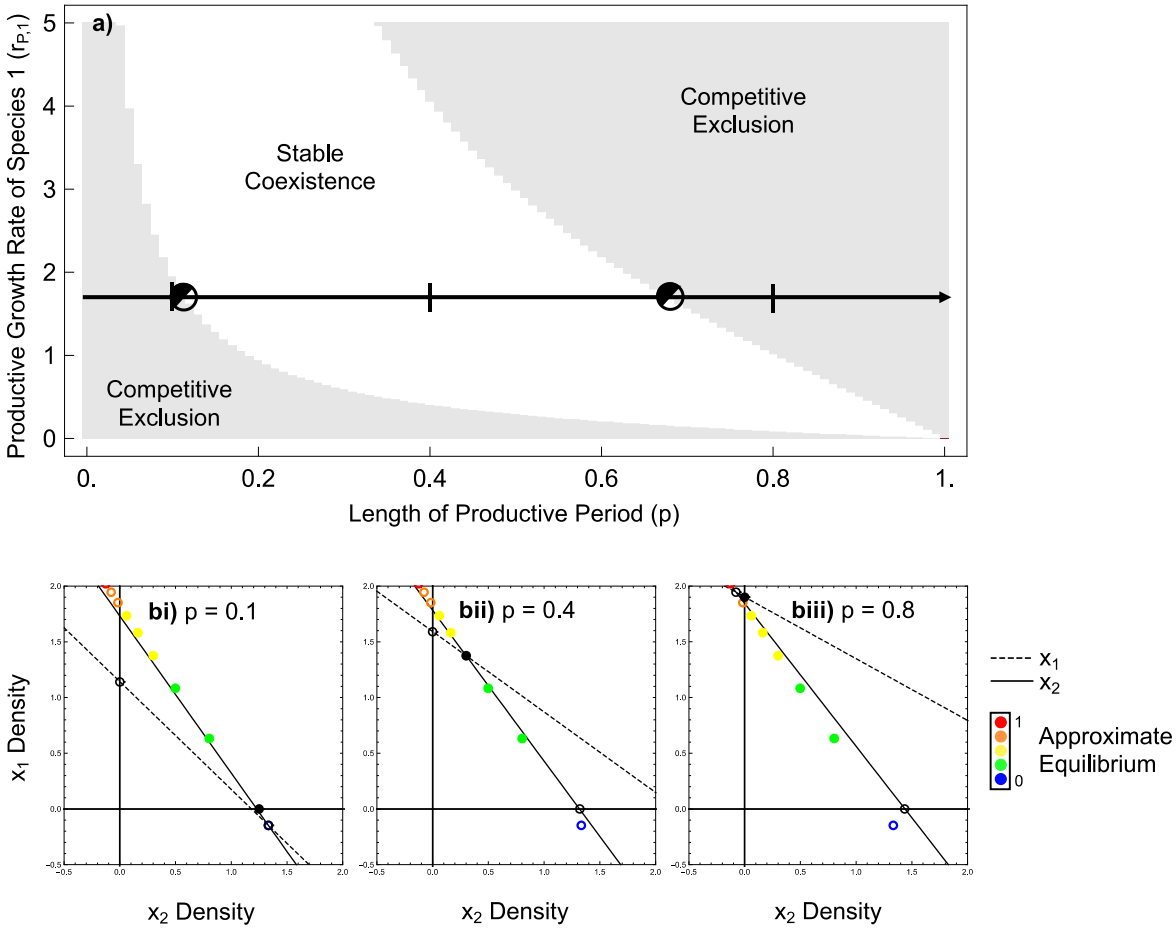
a)
Productive Growth Rate of Species 1 ($r_{P,1}$)
Length of Productive Period (p)
Stable Coexistence
Competitive Exclusion
Competitive Exclusion
bi) p = 0.1
bii) p = 0.4
biii) p = 0.8
x_1 Density
x_2 Density
x_1
x_2
Approximate Equilibrium

Figure 5

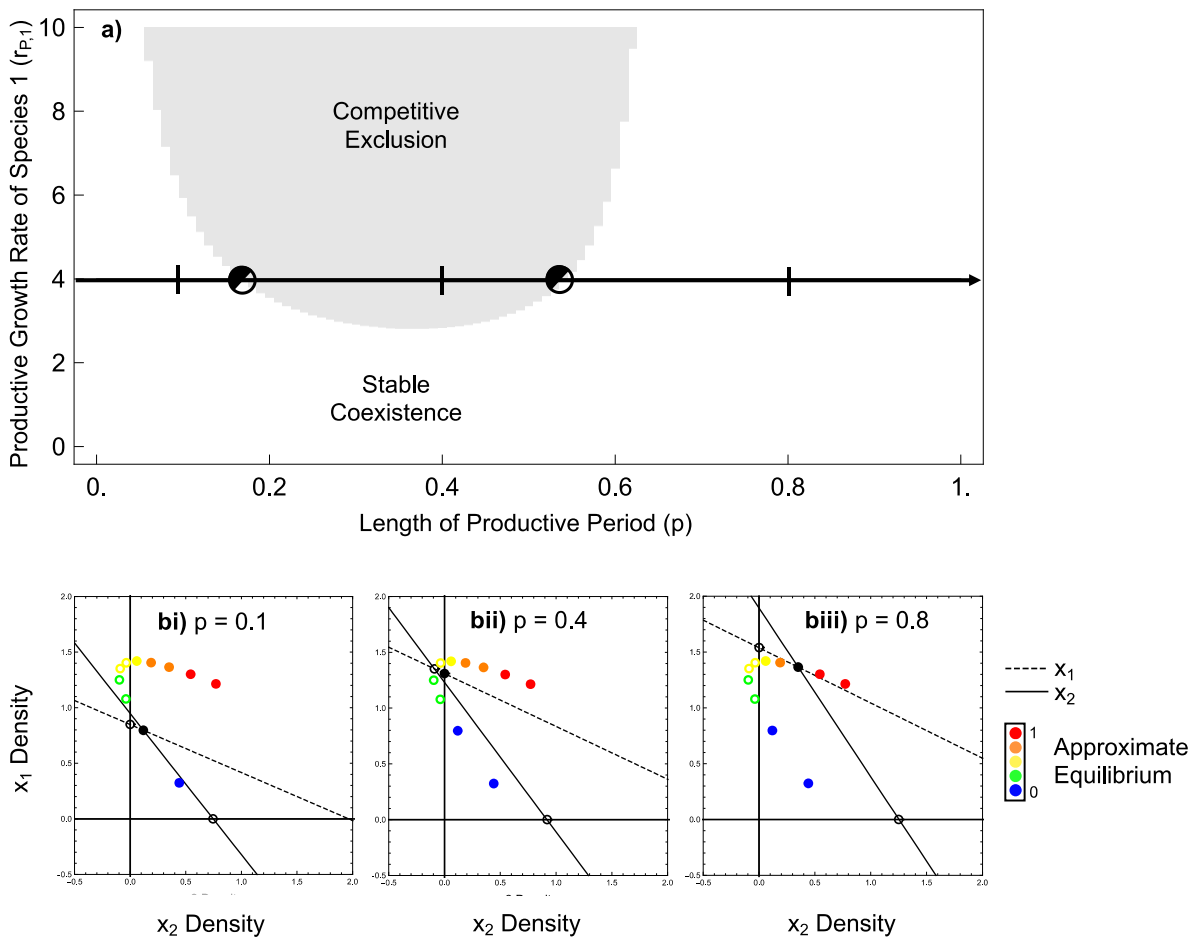
a)
Competitive Exclusion
Stable Coexistence
Productive Growth Rate of Species 1 ($r_{P,1}$)
Length of Productive Period (p)
bi) p = 0.1
bii) p = 0.4
biii) p = 0.8
x_1 Density
x_2 Density
x_1
x_2
Approximate Equilibrium

Figure

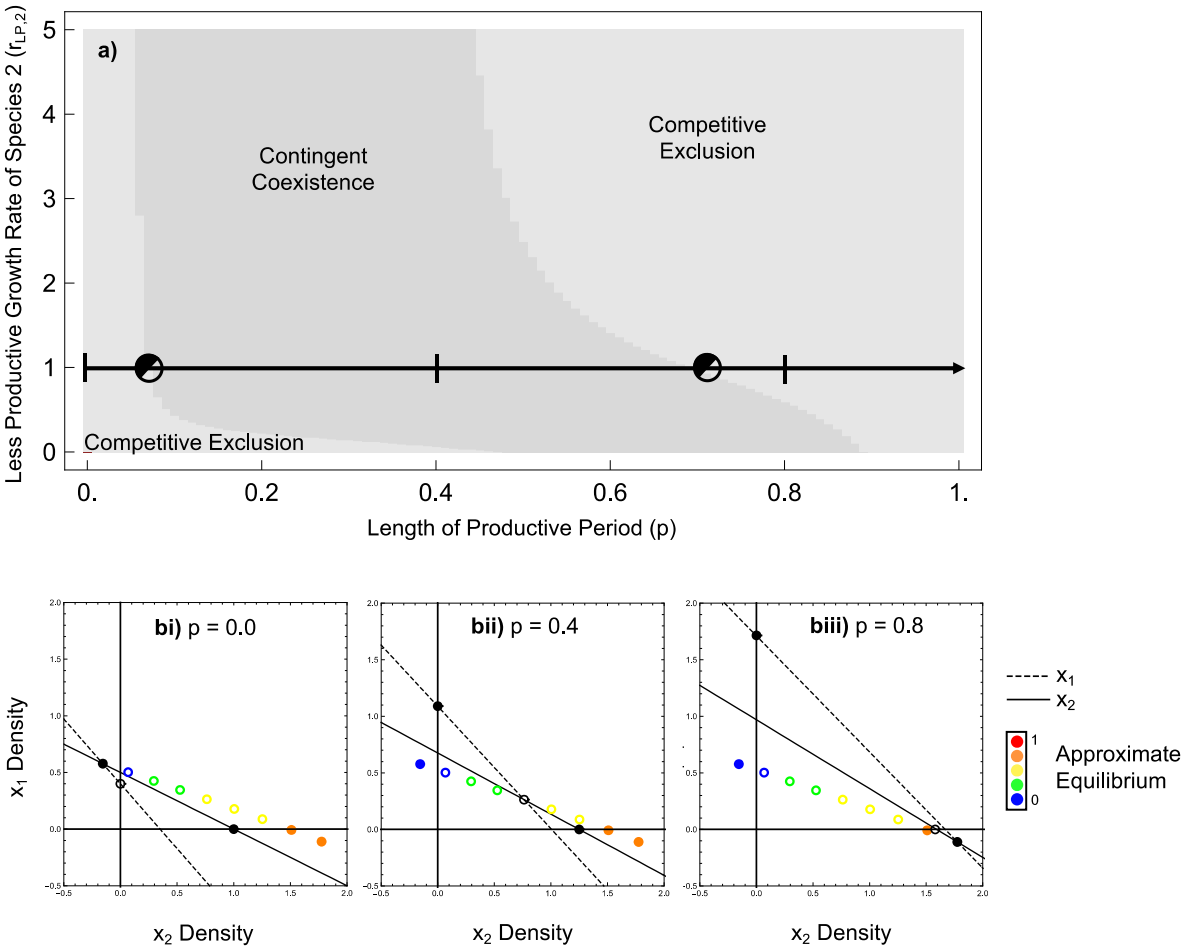
a)
Contingent Coexistence
Competitive Exclusion
Competitive Exclusion
Less Productive Growth Rate of Species 2 ($r_{LP,2}$)
Length of Productive Period (p)
bi) p = 0.0
bii) p = 0.4
biii) p = 0.8
x_1 Density
x_2 Density
x_1
x_2
Approximate Equilibrium
1
0

Coexistence in Periodic Environments: Supplementary Material

S1: A Linearization of the Periodic Lotka-Volterra Dynamics

If we consider any point on the phaseplane (X_j,X_k) due to the productive season that lasts from 0 to p where p is a fraction, then we know:

$$X_{P,j}(p) = X_{P,j}(0) + \int_0^p \frac{dX_{P,j}}{dt} dt \tag{1}$$

$$X_{P,k}(p) = X_{P,k}(0) + \int_0^p \frac{dX_{P,k}}{dt} dt \tag{2}$$

These dynamics follow the differential equation over the trajectory from 0 to p starting at the values $X_{P,j}(0)$. We linearize the trajectory over 0 to p by assuming the $\frac{dX_{P,j}}{dt}$ remains constant (e.g., we calculate the instantaneous $\frac{dX_{P,j}}{dt}$ for a point in the phaseplane, say for time (0)). As this is now a constant, we can use the Fundamental Theorem of Calculus to solve for Equations (1) and (2) above yielding:

$$X_{P,j}(p) - X_{P,j}(0) = \frac{dX_{P,j}}{dt} \; t \; \Big|_0^p \tag{3}$$

$$X_{P,j}(p) - X_{P,j}(0) = p\frac{dX_{P,j}}{dt} - 0\frac{dX_{P,j}}{dt} \tag{4}$$

$$X_{P,j}(p) - X_{P,j}(0) = p\frac{dX_{P,j}}{dt} \tag{5}$$

Similarly, we solve for the less productive season between p and 1, giving us:

$$X_{LP,j}(1) - X_{LP,j}(p) = (1-p)\frac{dX_{LP,j}}{dt} \tag{6}$$

Thus, the linearization estimates the trajectory as a linear scale movement following the length of the time interval (either *p*, or (1 – *p*)). We can take this simple estimate as a way to estimate the within seasonal dynamics and use them to estimate the periodic 0-isoclines.

Given Equations (5) and (6), the X_j isocline occurs when:

$$p\frac{dX_{P,j}}{dt} = -(1-p)\frac{dX_{LP,j}}{dt} \tag{7}$$

With this approximation, and for simplicity assuming no time dependency, we substitute the productive and less productive Lotka-Volterra models into equation (7):

$$p\ r_{P,j}X_j(1-\alpha_{P,jj}X_j-\alpha_{P,jk}X_k) = -(1-p)\ r_{LP,j}X_j(1-\alpha_{LP,jj}X_j-\alpha_{LP,jk}X_k) \tag{8}$$

We can now solve for the isocline solutions:

$$X_j = \frac{pr_{P,j}\alpha_{P,jk}-(1-p)r_{LP,j}\alpha_{LP,jk}}{pr_{P,j}\alpha_{P,jj}-(1-p)r_{LP,j}\alpha_{LP,jj}}X_k + \frac{pr_{P,j}+(1-p)r_{LP,j}}{pr_{P,j}\alpha_{P,jj}-(1-p)r_{LP,j}\alpha_{LP,jj}} \tag{9}$$

This isocline approximation, for both species, allows us to determine coexistence criteria for seasonal environments.

S2: Isocline Approximation and Numerical Simulation Comparison

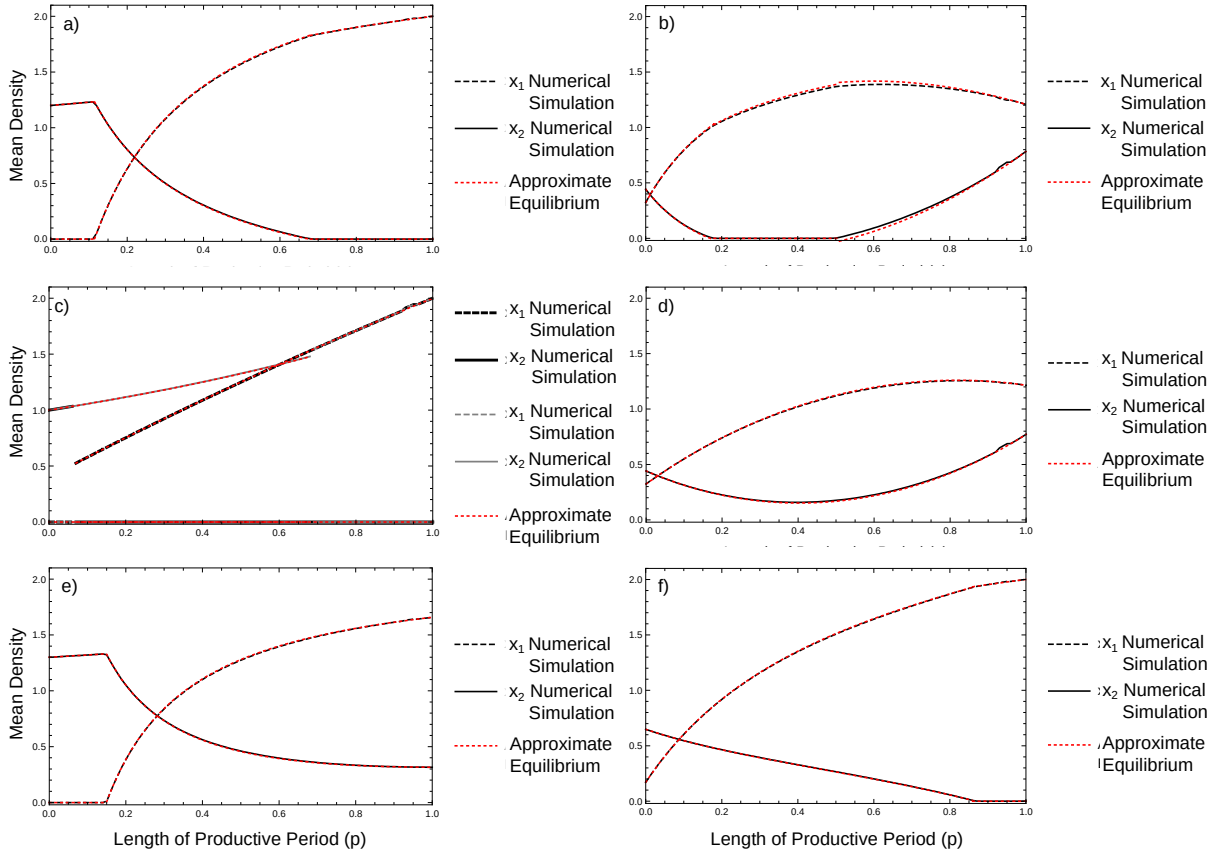

Figure S2.1: Comparison of Isocline Approximation against Numerical Simulations. White zone represents stable coexistence, light gray zone represents contingent coexistence, and dark gray zone represents contingent coexistence. a) Seasonally-mediated coexistence. Parametric values: $\alpha_{P,21}$=0.53, $\alpha_{P,12}$=0.25, $\alpha_{P,11}$=0.5, $\alpha_{P,22}$=0.66, $r_{P,1}$=1.7, $r_{P,2}$=1.2, $\alpha_{LP,21}$=0.583, $\alpha_{LP,12}$=1.22, $\alpha_{LP,11}$=1.11, $\alpha_{LP,22}$=0.83, $r_{LP,1}$=0.3, $r_{LP,2}$=1. b) Seasonally-mediated competitive exclusion. Parametric values: $\alpha_{P,21}$=0.4, $\alpha_{P,12}$=0.3125, $\alpha_{P,11}$=0.625, $\alpha_{P,22}$=0.66, $r_{P,1}$=4, $r_{P,2}$=1.2, $\alpha_{LP,21}$=1.14, $\alpha_{LP,12}$=0.8, $\alpha_{LP,11}$=2, $\alpha_{LP,22}$=1.43, $r_{LP,1}$=0.3, $r_{LP,2}$=1. c) Seasonally-mediated contingent coexistence. The equilibrium is unstable in the dark gray zone and multiple attractors exist between the two species. Parametric values; $\alpha_{P,21}$=0.83, $\alpha_{P,12}$=0.5, $\alpha_{P,11}$=0.5, $\alpha_{P,22}$=0.55, $r_{P,1}$=1.7, $r_{P,2}$=1.2,

$\alpha_{LP,21}$=2, $\alpha_{LP,12}$=2.86, $\alpha_{LP,11}$=2.5, $\alpha_{LP,22}$=1, $r_{LP,1}$=0.3, $r_{LP,2}$=1. d) Counterintuitive mean density change. Parametric values; $\alpha_{P,21}$=0.4, $\alpha_{P,12}$=0.31, $\alpha_{P,11}$=0.63, $\alpha_{P,22}$=0.67, $r_{P,1}$=1.7, $r_{P,2}$=1.2, $\alpha_{LP,21}$=1.14, $\alpha_{LP,12}$=0.8, $\alpha_{LP,11}$=2, $\alpha_{LP,22}$=1.43, $r_{LP,1}$=0.3, $r_{LP,2}$=1. e) Mean density change with competitive exclusion in the less productive season. Parametric values; $\alpha_{P,21}$=0.48, $\alpha_{P,12}$=0.25, $\alpha_{P,11}$=0.56, $\alpha_{P,22}$=0.67, $r_{P,1}$=1.7, $r_{P,2}$=1.2, $\alpha_{LP,21}$=0.59, $\alpha_{LP,12}$=1.25, $\alpha_{LP,11}$=1.11, $\alpha_{LP,22}$=0.77, $r_{LP,1}$=0.3, $r_{LP,2}$=1. f) Mean density change with competitive exclusion in the productive season. Parametric values; $\alpha_{P,21}$=0.53, $\alpha_{P,12}$=0.25, $\alpha_{P,11}$=0.5, $\alpha_{P,22}$=0.67, $r_{P,1}$=1.7, $r_{P,2}$=1.2, $\alpha_{LP,21}$=0.43, $\alpha_{LP,12}$=1.25, $\alpha_{LP,11}$=1.11, $\alpha_{LP,22}$=1.43, $r_{LP,1}$=0.3, $r_{LP,2}$=1.

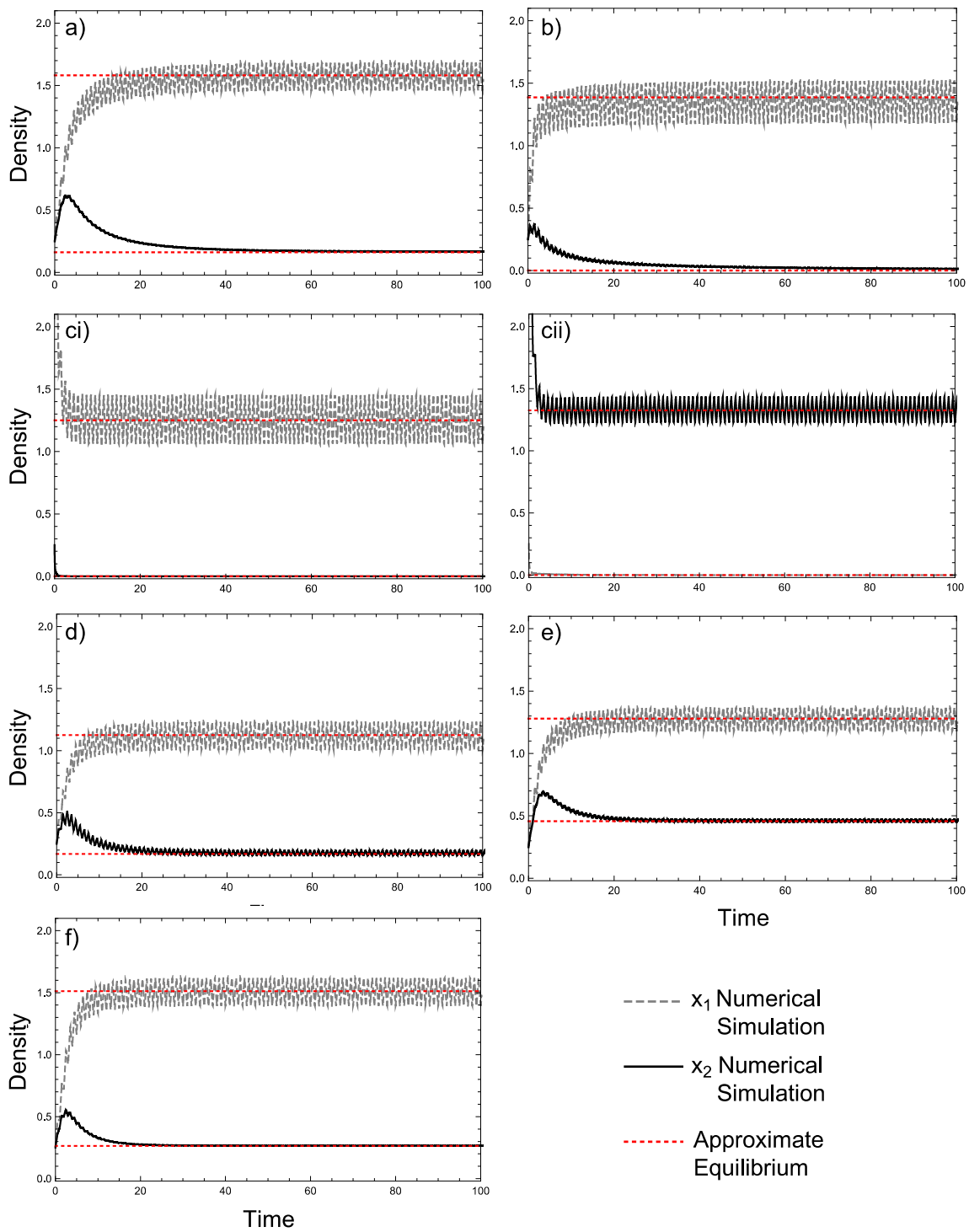

Figure S2.2: Time Series at p = 0.5 for the comparison of isocline approximation against numerical simulations. a) Seasonally-mediated coexistence. Parametric values:

$\alpha_{P,21}$=0.53, $\alpha_{P,12}$=0.25, $\alpha_{P,11}$=0.5, $\alpha_{P,22}$=0.66, $r_{P,1}$=1.7, $r_{P,2}$=1.2, $\alpha_{LP,21}$=0.583, $\alpha_{LP,12}$=1.22, $\alpha_{LP,11}$=1.11, $\alpha_{LP,22}$=0.83, $r_{LP,1}$=0.3, $r_{LP,2}$=1. b) Seasonally-mediated competitive exclusion. Parametric values: $\alpha_{P,21}$=0.53, $\alpha_{P,12}$=0.25, $\alpha_{P,11}$=0.5, $\alpha_{P,22}$=0.66, $r_{P,1}$=4, $r_{P,2}$=1.2, $\alpha_{LP,21}$=0.583, $\alpha_{LP,12}$=1.22, $\alpha_{LP,11}$=1.11, $\alpha_{LP,22}$=0.83, $r_{LP,1}$=0.3, $r_{LP,2}$=1. ci) Seasonally-mediated contingent coexistence. X_1 competitively excluded X_2. Parametric values; $\alpha_{P,21}$=0.83, $\alpha_{P,12}$=0.5, $\alpha_{P,11}$=0.5, $\alpha_{P,22}$=0.55, $r_{P,1}$=1.7, $r_{P,2}$=1.2, $\alpha_{LP,21}$=2, $\alpha_{LP,12}$=2.86, $\alpha_{LP,11}$=2.5, $\alpha_{LP,22}$=1, $r_{LP,1}$=0.3, $r_{LP,2}$=1. cii) Seasonally-mediated contingent coexistence. X_2 competitively excluded X_1. Parametric values; $\alpha_{P,21}$=0.83, $\alpha_{P,12}$=0.5, $\alpha_{P,11}$=0.5, $\alpha_{P,22}$=0.55, $r_{P,1}$=1.7, $r_{P,2}$=1.2, $\alpha_{LP,21}$=2, $\alpha_{LP,12}$=2.86, $\alpha_{LP,11}$=2.5, $\alpha_{LP,22}$=1, $r_{LP,1}$=0.3, $r_{LP,2}$=1. d) Counterintuitive mean density change. Parametric values; $\alpha_{P,21}$=0.4, $\alpha_{P,12}$=0.31, $\alpha_{P,11}$=0.63, $\alpha_{P,22}$=0.67, $r_{P,1}$=1.7, $r_{P,2}$=1.2, $\alpha_{LP,21}$=1.14, $\alpha_{LP,12}$=0.8, $\alpha_{LP,11}$=2, $\alpha_{LP,22}$=1.43, $r_{LP,1}$=0.3, $r_{LP,2}$=1. e) Mean density change with competitive exclusion in the less productive season. Parametric values; $\alpha_{P,21}$=0.48, $\alpha_{P,12}$=0.25, $\alpha_{P,11}$=0.56, $\alpha_{P,22}$=0.67, $r_{P,1}$=1.7, $r_{P,2}$=1.2, $\alpha_{LP,21}$=0.59, $\alpha_{LP,12}$=1.25, $\alpha_{LP,11}$=1.11, $\alpha_{LP,22}$=0.77, $r_{LP,1}$=0.3, $r_{LP,2}$=1. f) Mean density change with competitive exclusion in the productive season. Parametric values; $\alpha_{P,21}$=0.53, $\alpha_{P,12}$=0.25, $\alpha_{P,11}$=0.5, $\alpha_{P,22}$=0.67, $r_{P,1}$=1.7, $r_{P,2}$=1.2, $\alpha_{LP,21}$=0.43, $\alpha_{LP,12}$=1.25, $\alpha_{LP,11}$=1.11, $\alpha_{LP,22}$=1.43, $r_{LP,1}$=0.3, $r_{LP,2}$=1.

S3: Generality of Results for all Seasonally-Mediated Competitive Outcomes Using Isocline Approach

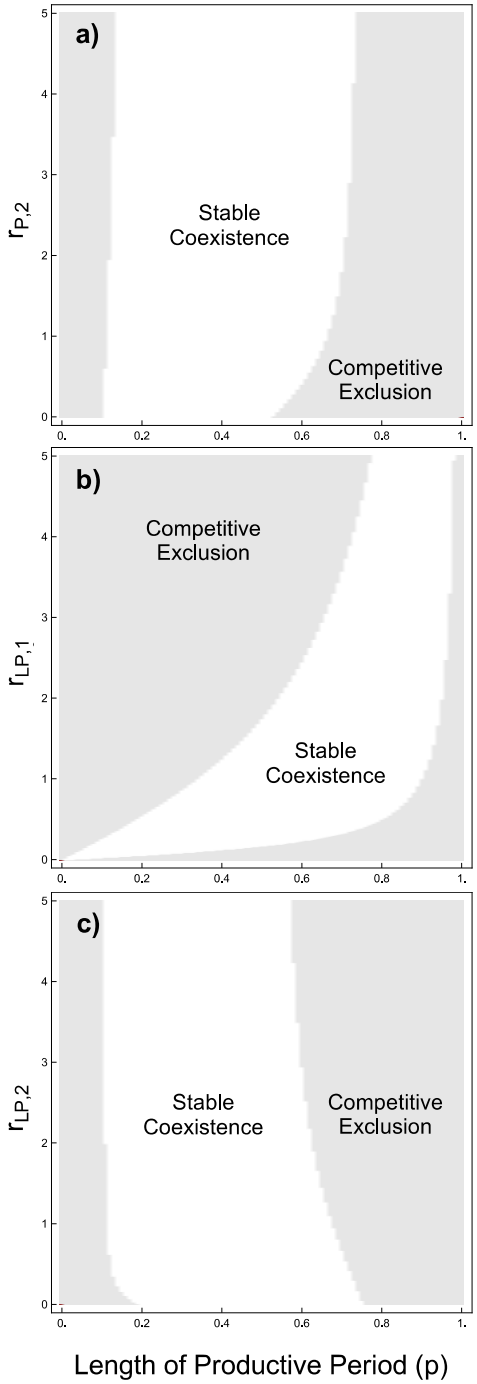

Figure S3.1.1: Two-dimensional bifurcation diagrams of seasonally-mediated coexistence across other growth rate parameters. Seasonally-mediated coexistence expending over a wide range of possible growth rate values. a) Species 2's productive growth rate. b) Species 1's less productive growth rate. c) Species 2's less productive growth rate. Parametric values: $\alpha_{P,21}$=0.53, $\alpha_{P,12}$=0.25, $\alpha_{P,11}$=0.5, $\alpha_{P,22}$=0.66, $r_{P,1}$=1.7, $r_{P,2}$=1.2, $\alpha_{LP,21}$=0.583, $\alpha_{LP,12}$=1.22, $\alpha_{LP,11}$=1.11, $\alpha_{LP,22}$=0.83, $r_{LP,1}$=0.3, $r_{LP,2}$=1.

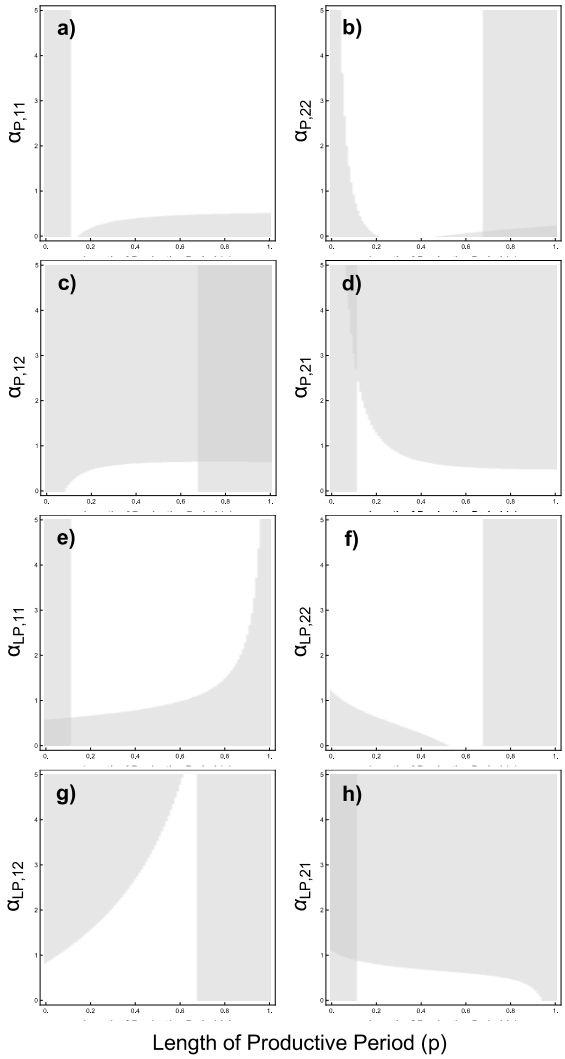

Figure S3.1.2: Seasonally-mediated coexistence bifurcation diagrams for inter- and intraspecific competition coefficients: Seasonally-mediated coexistence expending over a wide range of possible inter- and intraspecific competitive coefficients. White zone represents stable coexistence, light gray zone represents competitive exclusion, and dark gray region represents contingent coexistence. a) Species 1's productive intraspecific competitive coefficient. b) Species 2's productive intraspecific competitive coefficient. c) Productive interspecific competitive coefficient of species 2 on species 1. d) Productive interspecific competitive coefficient of species 1 on species 2. e) Species 1's less productive intraspecific competitive coefficient. f) Species 2's less productive intraspecific competitive coefficient. g) Less productive interspecific competitive coefficient of species 2 on species 1. g) Less productive interspecific competitive coefficient of species 1 on species 2. Parametric values: $\alpha_{P,21}$=0.53, $\alpha_{P,12}$=0.25, $\alpha_{P,11}$=0.5, $\alpha_{P,22}$=0.66, $r_{P,1}$=1.7, $r_{P,2}$=1.2, $\alpha_{LP,21}$=0.583, $\alpha_{LP,12}$=1.22, $\alpha_{LP,11}$=1.11, $\alpha_{LP,22}$=0.83, $r_{LP,1}$=0.3, $r_{LP,2}$=1.

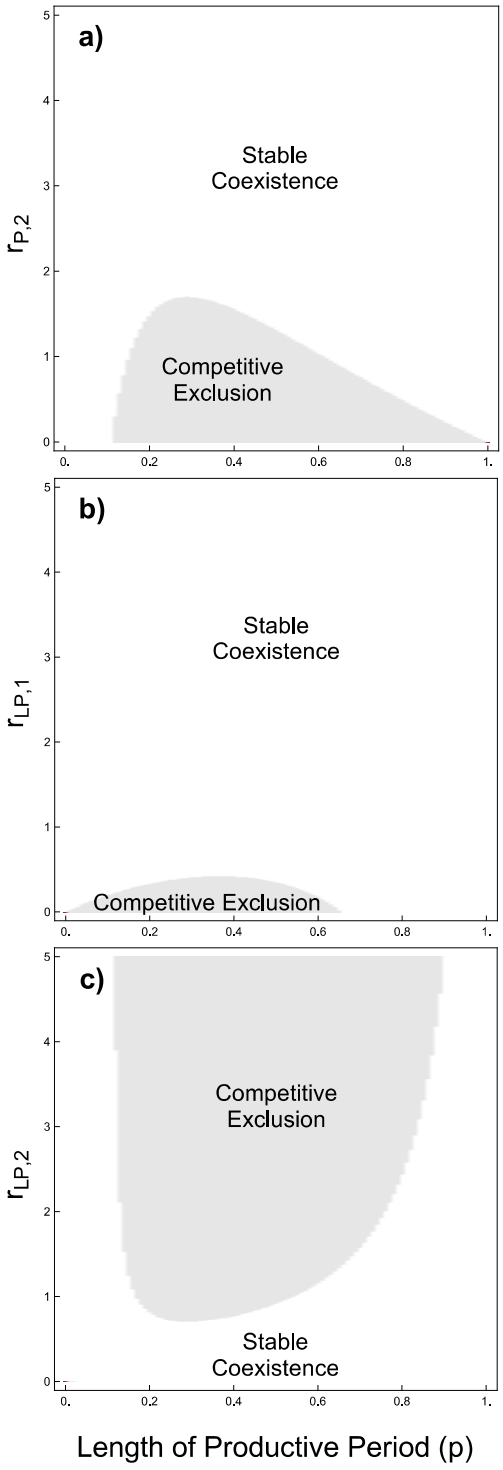

Figure S3.2.1: Two-dimensional bifurcation diagrams of seasonally-mediated competitive exclusion across other growth rate parameters. Seasonally-mediated competitive exclusion expending over a wide range of possible growth rate values. a) Species 2's productive growth rate. b) Species 1's less productive growth rate. c) Species 2's less productive growth rate. Parametric values: Parametric values: $\alpha_{P,21}$=0.4, $\alpha_{P,12}$=0.3125, $\alpha_{P,11}$=0.625, $\alpha_{P,22}$=0.66, r_{P1j}=4, $r_{P,2}$=1.2, $\alpha_{L,P21}$=1.14, $\alpha_{LP,12}$=0.8, $\alpha_{LP,11}$=2, $\alpha_{LP,22}$=1.43 $r_{LP,1}$=0.3, $r_{LP,2}$=1.

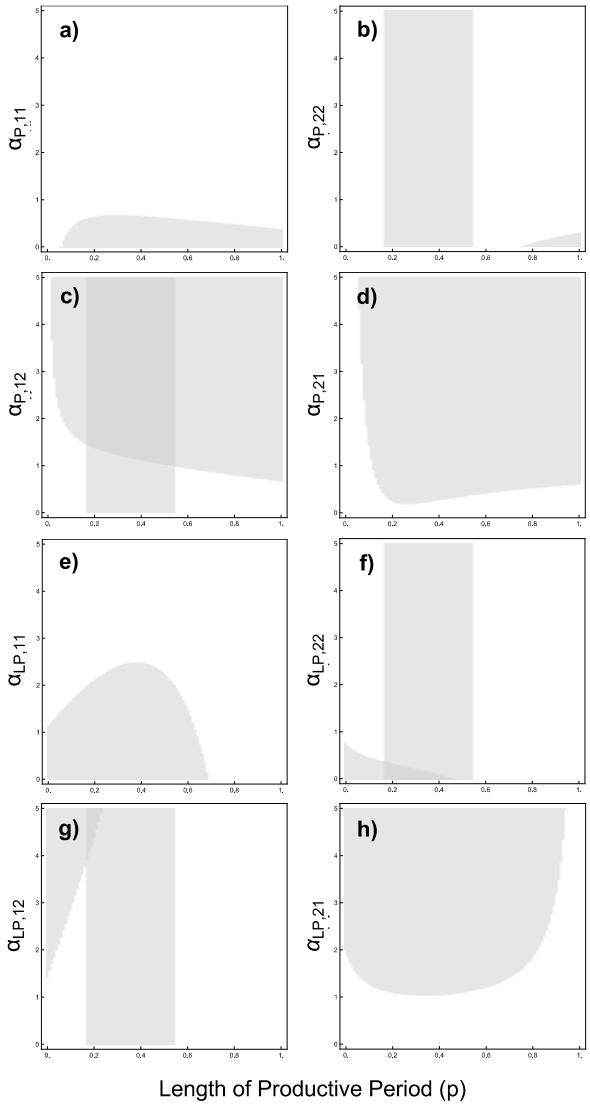

Figure S3.2.2: Seasonally-mediated competitive exclusion bifurcation diagrams for inter- and intraspecific competition coefficients: Seasonally-mediated competitive exclusion expending over a wide range of possible inter- and intraspecific competitive coefficients. White zone represents stable coexistence, light gray zone represents competitive exclusion, and dark gray region represents contingent coexistence. a) Species 1's productive intraspecific competitive coefficient. b) Species 2's productive intraspecific competitive coefficient. c) Productive interspecific competitive coefficient of species 2 on species 1. d) Productive interspecific competitive coefficient of species 1 on species 2. e) Species 1's less productive intraspecific competitive coefficient. f) Species 2's less productive intraspecific competitive coefficient. g) Less productive interspecific competitive coefficient of species 2 on species 1. g) Less productive interspecific competitive coefficient of species 1 on species 2. Parametric values: $\alpha_{P,21}$=0.4, $\alpha_{P,12}$=0.3125, $\alpha_{P,11}$=0.625, $\alpha_{P,22}$=0.66, $r_{P,1}$=4, $r_{P,2}$=1.2, $\alpha_{LP,21}$=1.14, $\alpha_{LP,12}$=0.8, $\alpha_{LP,11}$=2, $\alpha_{LP,22}$=1.43 $r_{LP,1}$=0.3, $r_{LP,2}$=1.

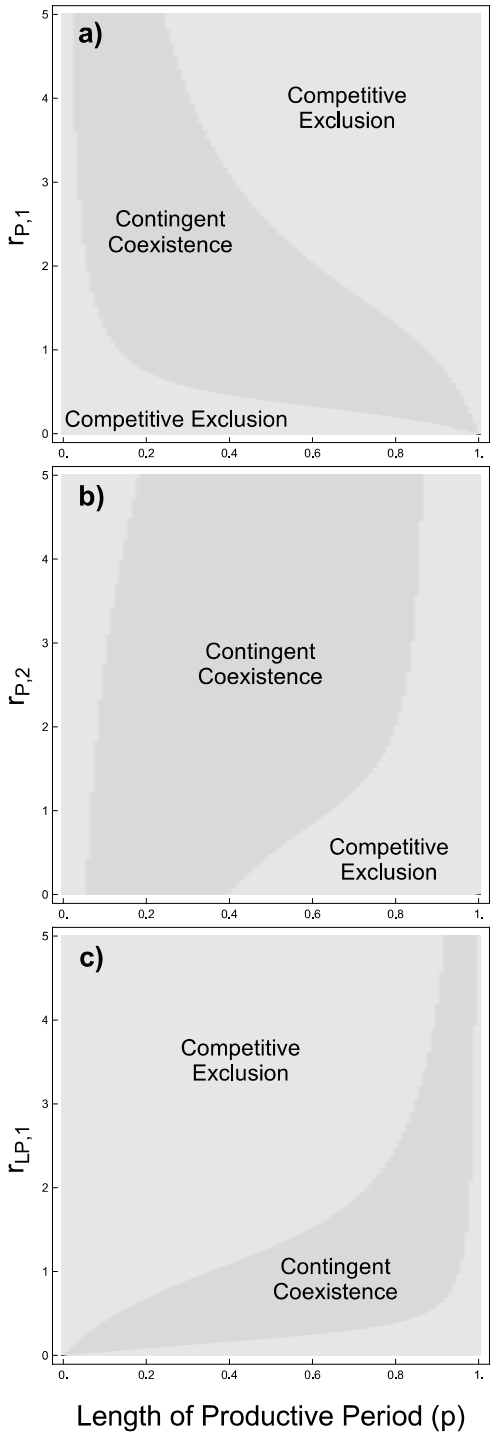

Figure S3.3.1: Two-dimensional bifurcation diagrams of seasonally-mediated contingent coexistence across other growth rate parameters. Seasonally-mediated contingent coexistence expending over a wide range of possible growth rate values. a) Species 1's productive growth rate. b) Species 2's productive growth rate. c) Species 1's less productive growth rate. Parametric values; $\alpha_{P,21}$=0.83, $\alpha_{P,12}$=0.5, $\alpha_{P,11}$=0.5, $\alpha_{P,22}$=0.55, $r_{P,1}$=1.7, $r_{P,2}$=1.2, $\alpha_{LP,21}$=2, $\alpha_{LP,12}$=2.86, $\alpha_{LP,11}$=2.5, $\alpha_{LP,22}$=1, $r_{LP,1}$=0.3, $r_{LP,2}$=1.

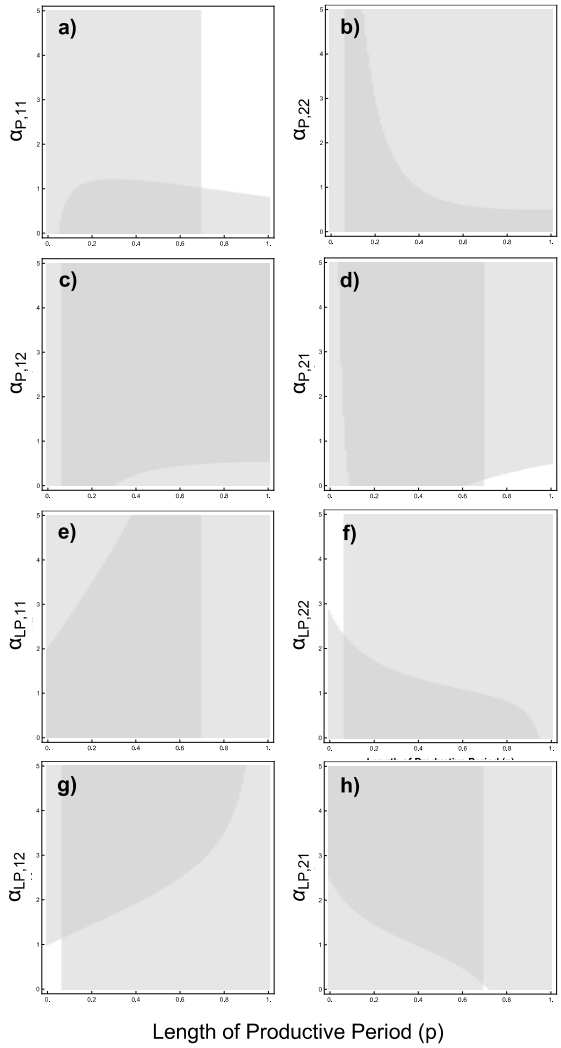

Figure S3.3.2: Seasonally-mediated contingent coexistence bifurcation diagrams for inter- and intraspecific competition coefficients: Seasonally-mediated contingent coexistence expending over a wide range of possible inter- and intraspecific competitive coefficients. White zone represents stable coexistence, light gray zone represents competitive exclusion, and dark gray region represents contingent coexistence. a) Species 1's productive intraspecific competitive coefficient. b) Species 2's productive intraspecific competitive coefficient. c) Productive interspecific competitive coefficient of species 2 on species 1. d) Productive interspecific competitive coefficient of species 1 on species 2. e) Species 1's less productive intraspecific competitive coefficient. f) Species 2's less productive intraspecific competitive coefficient. g) Less productive interspecific competitive coefficient of species 2 on species 1. g) Less productive interspecific competitive coefficient of species 1 on species 2. Parametric values; $\alpha_{P,21}$=0.83, $\alpha_{P,12}$=0.5, $\alpha_{P,11}$=0.5, $\alpha_{P,22}$=0.55, $r_{P,1}$=1.7, $r_{P,2}$=1.2, $\alpha_{LP,21}$=2, $\alpha_{LP,12}$=2.86, $\alpha_{LP,11}$=2.5, $\alpha_{LP,22}$=1, $r_{LP,1}$=0.3, $r_{LP,2}$=1.

S4: Tracking Isocline Approximation across Productivity Length for all Seasonally-Mediated Competitive Outcomes

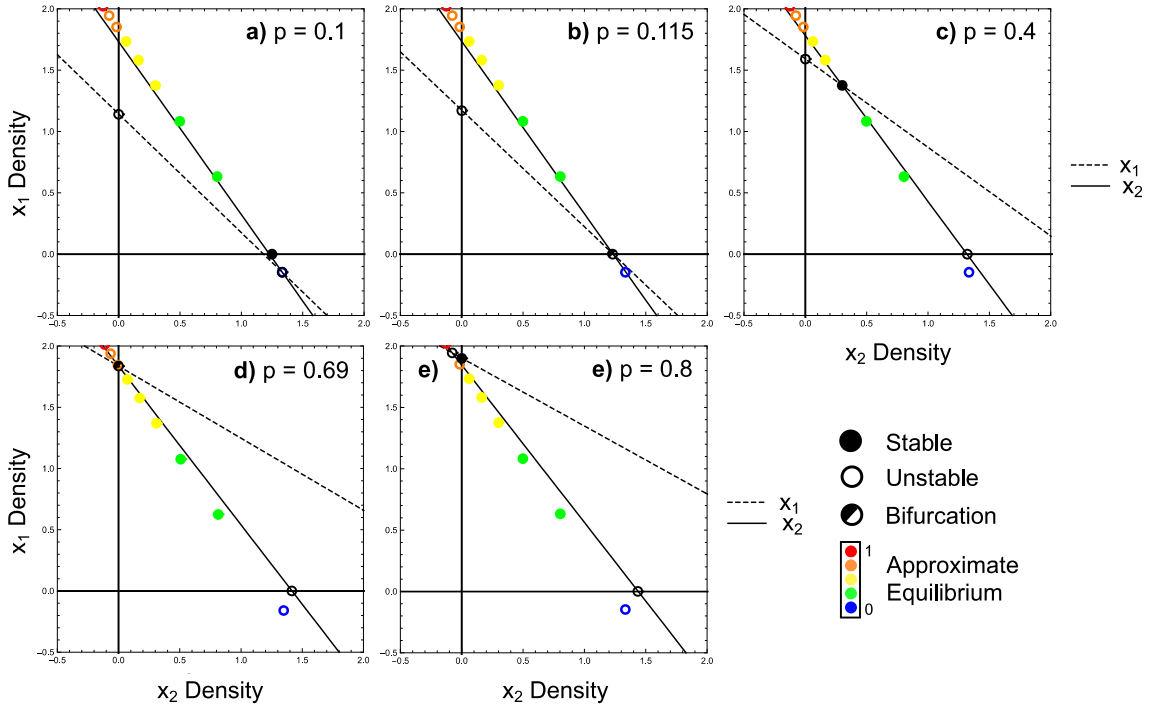

Figure S4.1: Seasonally-mediated coexistence isocline approximation. Isocline approximation tracking the interior equilibrium as the productive season increases in length from a) p=0.1; competitive exclusion, to b) p=0.115; transcritical bifurcation, to c) p=0.4; stable coexistence, to d) p=0.69; transcritical bifurcation, to e) p=0.8; competitive exclusion. Parametric values: $\alpha_{P,21}$=0.53, $\alpha_{P,12}$=0.25, $\alpha_{P,11}$=0.5, $\alpha_{P,22}$=0.66, $r_{P,1}$=1.7, $r_{P,2}$=1.2, $\alpha_{LP,21}$=0.583, $\alpha_{LP,12}$=1.22, $\alpha_{LP,11}$=1.11, $\alpha_{LP,22}$=0.83, $r_{LP,1}$=0.3, $r_{LP,2}$=1.

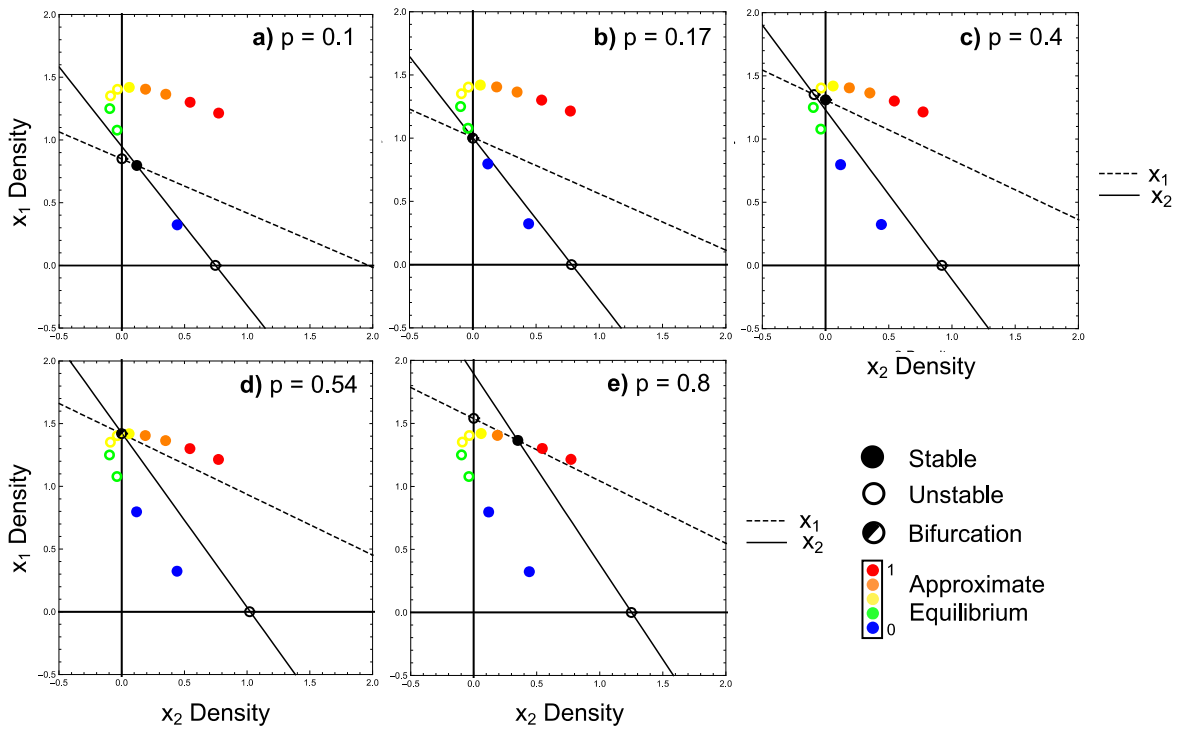

Figure S4.2: Seasonally-mediated competitive exclusion isocline approximation. Isocline approximation tracking the interior equilibrium as the productive season increases in length from a) p=0.1; stable coexistence, to b) p=0.17; transcritical bifurcation, to c) p=0.4; competitive exclusion, to d) p=0.54; transcritical bifurcation, to e) p=0.8; stable coexistence. Parametric values: $\alpha_{P,21}$=0.4, $\alpha_{P,12}$=0.3125, $\alpha_{P,11}$=0.625, $\alpha_{P,22}$=0.66, $r_{P,1}$=4, $r_{P,2}$=1.2, $\alpha_{LP,21}$=1.14, $\alpha_{LP,12}$=0.8, $\alpha_{LP,11}$=2, $\alpha_{LP,22}$=1.43 $r_{LP,1}$=0.3, $r_{LP,2}$=1.

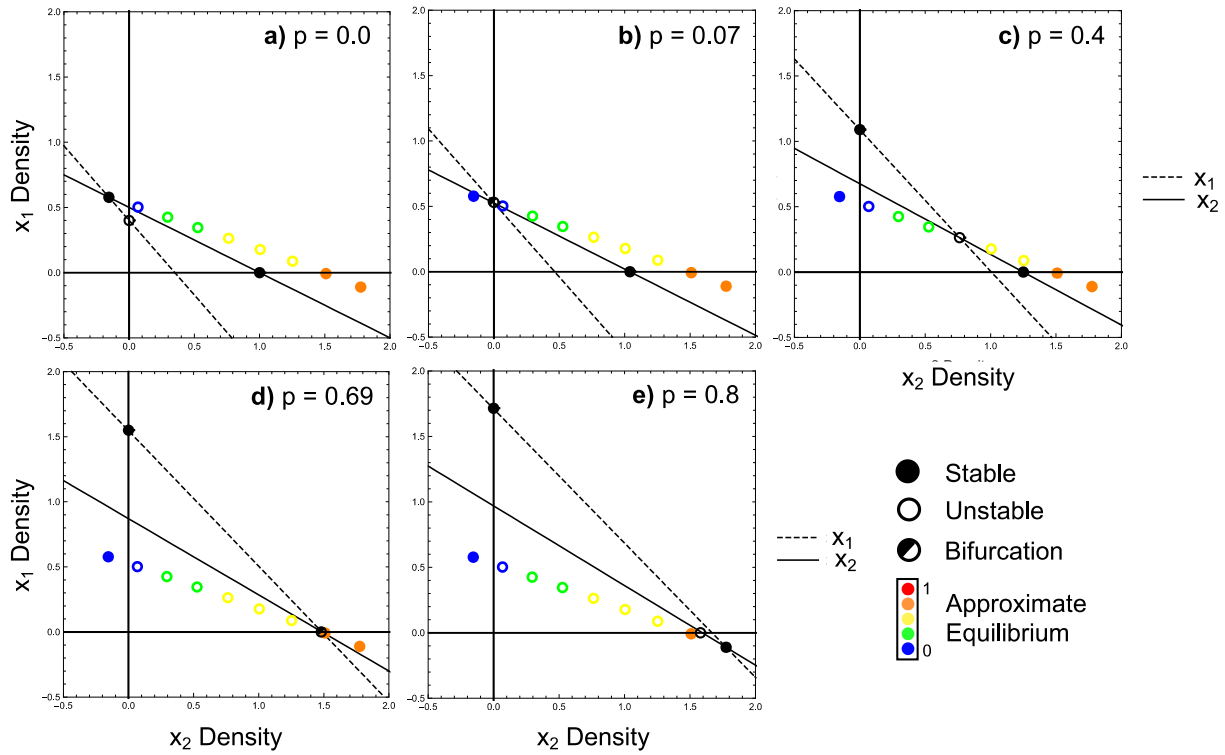

Figure S4.3: Seasonally-mediated contingent coexistence isocline approximation. Isocline approximation tracking the interior equilibrium as the productive season increases in length from a) p=0.0; competitive exclusion, to b) p=0.07; transcritical bifurcation, to c) p=0.4; contingent coexistence, to d) p=0.69; transcritical bifurcation, to e) p=0.8; competitive exclusion. Parametric values; $\alpha_{P,21}$=0.83, $\alpha_{P,12}$=0.5, $\alpha_{P,11}$=0.5, $\alpha_{P,22}$=0.55, $r_{P,1}$=1.7, $r_{P,2}$=1.2, $\alpha_{LP,21}$=2, $\alpha_{LP,12}$=2.86, $\alpha_{LP,11}$=2.5, $\alpha_{LP,22}$=1, $r_{LP,1}$=0.3, $r_{LP,2}$=1.

S5: Approximation Breakdown

Our results hold for a very broad range in growth rates (e.g., r = 0.0 to 10.0). However, recognizing that linear assumptions may be weekend when numerical assumptions become nonlinear, we push growth rates to see if the approximation becomes inaccurate. Below we show that indeed it can breakdown but occurs when all growth rates become incredibly larger (i.e., all r's x10 units) compared to the inter- and intraspecific competition coefficients. Even here, the approximation remains to be a reasonably good qualitative predictor of steady state behaviour for seasonally-mediated coexistence and contingent coexistent (Figure S5bi and ci respectively), except for cases of seasonally-mediated competitive exclusion (Figure S5ai).

In Figure S5ai, the approximation still assumes seasonally-mediated competitive exclusion, even when species coexist throughout the entire length of the productive period (p). When species growth rates are multiplied by 10 units, these faster growth rates result in densities spending more time at or near each seasonal equilibrium and therefore, there are more nonlinear changes within each season – causing the linear assumption to fail. At lower r's, the densities remain in phase space between the two seasonal equilibria (since there is less rapid movement), and in these cases, the coupling of seasonal non-local dynamics can drive the system away from either equilibrium and towards competitive exclusion (i.e., as seen in Figure S5ai).

For seasonally-mediated coexistence (Figure S5bi) and contingent coexistence (Figure S5ci), when growth rates are multiplied by 10 units, the approximation still accurately

calculates the qualitative behaviour and bifurcations remarkably well. In both cases, as the rates of change become faster and more nonlinear with larger growth rates, species' densities reach their seasonal equilibrium much quicker and therefore spend more time at these specific densities (Figures S5bii and S5cii). Here, the asymptotic mean densities may skew closer toward a specific seasonal equilibrium and away from the approximation which can only calculate the average densities from the linear movements between the two seasons.

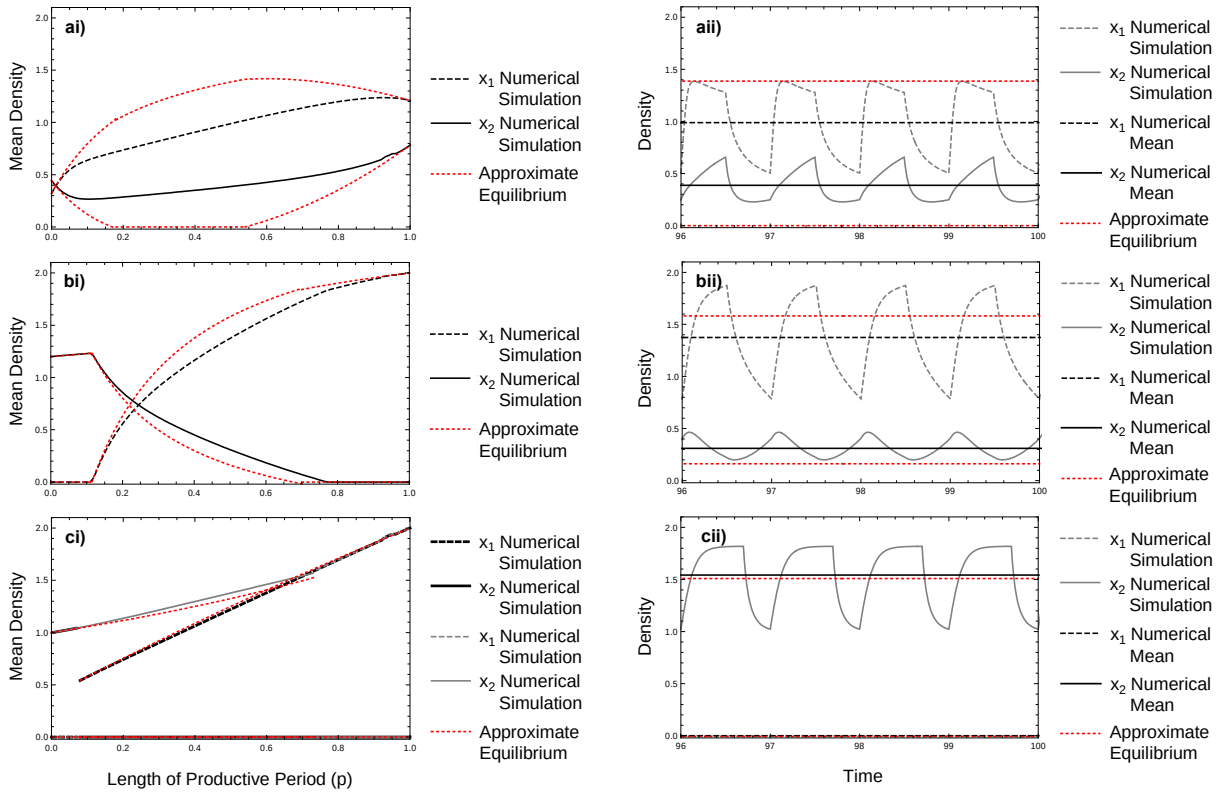

Figure S5: Isocline approximation breakdown. All growth rates for each of the seasonally-mediated outcomes are multiplied by 10 units to test the approximation's accuracy. In all mean density plots over the length of the productive period (*p*), white zones represent coexistence, light gray zones represent competitive exclusion, dark gray zones represent contingent coexistence. In all time series, white zones represent the productive period (*p*) and gray zones represent the less productive period (1-*p*). ai) Isocline approximation inaccurately assumes seasonally-mediated competitive exclusion when mean densities remain at coexistence throughout the entire productive period length. aii) Time series of nonlinear rates of change at mean asymptotic density when p=0.5. Parametric values: $\alpha_{P,21}$=0.4, $\alpha_{P,12}$=0.3125, $\alpha_{P,11}$=0.625, $\alpha_{P,22}$=0.66, $r_{P,1}$=40, $r_{P,2}$=12, $\alpha_{LP,21}$=1.14, $\alpha_{LP,12}$=0.8, $\alpha_{LP,11}$=2, $\alpha_{LP,22}$=1.43 $r_{LP,1}$=3, $r_{LP,2}$=10. bi) Isocline

approximation tracks qualitative behaviour and bifurcation points fairly well for seasonally-mediated coexistence. bii) Time series of nonlinear rates of change at mean asymptotic density when p=0.5. Parametric values: $\alpha_{P,21}$=0.53, $\alpha_{P,12}$=0.25, $\alpha_{P,11}$=0.5, $\alpha_{P,22}$=0.66, $r_{P,1}$=17, $r_{P,2}$=12, $\alpha_{LP,21}$=0.583, $\alpha_{LP,12}$=1.22, $\alpha_{LP,11}$=1.11, $\alpha_{LP,22}$=0.83, $r_{LP,1}$=3, $r_{LP,2}$=10. ci) Isocline approximation accurately tracks qualitative behaviour and bifurcation points for seasonally-mediate contingent coexistence. cii) Time series of nonlinear rates of change at mean asymptotic density when p=0.7. Parametric values; $\alpha_{P,21}$=0.83, $\alpha_{P,12}$=0.5, $\alpha_{P,11}$=0.5, $\alpha_{P,22}$=0.55, $r_{P,1}$=17, $r_{P,2}$=12, $\alpha_{LP,21}$=2, $\alpha_{LP,12}$=2.86, $\alpha_{LP,11}$=2.5, $\alpha_{LP,22}$=1, $r_{LP,1}$=3, $r_{LP,2}$=10.